

## Supporting Information

# Gels of Shape-Persistent Macrocycles: the Role of the Interior

Joscha Vollmeyer,<sup>1)</sup> Stefan-S. Jester,<sup>1)</sup> Friederike Eberhagen,<sup>1)</sup> Thomas Prangenberg,<sup>2)</sup> Werner  
Mader,<sup>2)</sup> and Sigurd Höger<sup>1)\*</sup>

<sup>1)</sup> *Kekulé-Institut für Organische Chemie und Biochemie,  
Rheinische Friedrich-Wilhelms-Universität Bonn, Gerhard-Domagk-Str. 1, 53121 Bonn,  
Germany.*

<sup>2)</sup> *Institut für Anorganische Chemie,  
Rheinische Friedrich-Wilhelms-Universität Bonn, Römerstraße 164, 53117 Bonn, Germany.*

<sup>\*)</sup> *Corresponding authors.*

*E-mail: stefan.jester@uni-bonn.de; hoeger@uni-bonn.de*

## Content

1	General methods.....	S3
1.1	Materials and equipment.....	S3
1.2	Scanning probe microscopy .....	S3
1.3	Transmission electron microscopy.....	S4
1.4	UV/vis spectroscopy.....	S4
1.5	Differential scanning calorimetry.....	S5
1.6	Polarized optical microscopy.....	S6
2	Molecular models.....	S7
3	Atomic force microscopy.....	S8
3.1	AFM images obtained from the gels .....	S8
3.2	AFM images of aggregates cast from solution .....	S13
4	Transmission electron microscopy.....	S15
5	UV/vis spectroscopy.....	S17
6	Differential scanning calorimetry.....	S18
7	Polarized optical microscopy.....	S19
8	Synthesis.....	S20
8.1	Overview.....	S20
8.2	Synthesis and characterization of building blocks 7, 9, 10.....	S23
8.3	Synthesis and characterization of macrocycles 1 and 3.....	S32
8.4	Synthesis and characterization of macrocycle 2 .....	S46
	References.....	S54

## 1 General methods

### 1.1 Materials and equipment

THF was dried over Na and benzophenone. Piperidine and pyridine were dried over CaH<sub>2</sub>. The anhydrous solvents were distilled and stored under argon if necessary. Reagents were purchased at reagent grade from commercial sources and used without further purification. **4**,<sup>[1]</sup> **8**,<sup>[2]</sup> and [(3-cyanopropyl)dimethylsilyl] (CPDMS) acetylene<sup>[3]</sup> were prepared according to literature procedures (cf. pp. S26 ff). All air-sensitive reactions were carried out using standard Schlenk techniques under argon. Analytical thin layer chromatography (TLC) was performed using precoated TLC plates (obtained from Macherey-Nagel, Alugram® SIL G/UV<sub>254</sub>, 0.2 mm). Column chromatography was performed using silica gel 60 M (Macherey-Nagel, 0.04 - 0.063 mm, 230 - 400 mesh) as stationary phase. <sup>1</sup>H and <sup>13</sup>C NMR spectra were recorded on Bruker DPX 300 (<sup>1</sup>H, 300 MHz; <sup>13</sup>C, 75 MHz), DPX 400 (<sup>1</sup>H, 400 MHz; <sup>13</sup>C, 100 MHz), and DPX 500 (<sup>1</sup>H, 500 MHz; <sup>13</sup>C, 125 MHz) spectrometers. Chemical shifts are reported as δ values (ppm) and referenced to residual <sup>1</sup>H or <sup>13</sup>C signals in deuterated solvents. Electron impact ionization (EI) mass spectroscopy (MS) was performed using a Finnigan ThermoQuest MAT 95 XL mass spectrometer. Matrix-assisted laser desorption/ionization (MALDI) MS was performed using a Bruker Daltonics autoflex II TOF/TOF. Electrospray ionization (ESI) MS data were recorded on a Bruker Daltonics ESI micrOTOF-Q instrument. Melting points were either determined using a Leica DMLB microscope with a hot stage and a home-built control unit, or by differential scanning calorimetry (DSC) using a Mettler Toledo DSC 823<sup>e</sup>. Gel permeation chromatography (GPC) was performed in THF (HPLC grade, stabilized with 2.5 ppm BHT) at room temperature. A Shimadzu recycling GPC system, equipped with an LC-20 AD pump, an SPD-20 A UV-detector, and a set of three preparative columns (obtained from PSS Polymer Standards Service, 10<sup>3</sup> Å, 5μ, 20 mm × 300 mm) was used for the purification of **1**, **2**, and **3**. The system was operated at a flow rate of 5 mL min<sup>-1</sup>.

### 1.2 Scanning probe microscopy

The experimental setup consists of an Agilent 5500 system placed on a Halcyonics active vibration damping platform, and is surrounded by a home-built acoustic damping box.

Atomic force microscopy (AFM) investigation of the aggregates of **1-3** was performed after depositing the latter onto freshly cleaved mica substrates. Depending on the consistence of the materials (varying with the concentration, i.e. gel or solution), two different sample preparation techniques were used. Aggregates obtained from gels were imaged after depositing and slightly

spreading the gel material onto mica by spin-coating using a Novocontrol SCE-10 spin coater and drying the sample in air. Aggregates from diluted solutions were imaged after dip-coating onto a freshly cleaved piece of mica and subsequent drying in air. All AFM experiments were carried out using Mikro Masch NSC15 cantilevers (tip radius < 10 nm, nominal force constant 40 N/m).

Scanning tunneling microscopy (STM) was performed at the solution/solid interface under ambient conditions. Typically, 1  $\mu$ L of a  $10^{-5}$ – $10^{-6}$  M solution of the respective substance in 1,2,4-trichlorobenzene (TCB) was dropped onto a piece of freshly cleaved highly oriented pyrolytic graphite (HOPG, SPI Inc., SPI-II quality) at elevated temperature (70 °C), and the sample was allowed to cool to r.t. prior to STM imaging. All STM measurements were performed *in situ* (with the tip immersed into the liquid) and typically completed within 30 min after the sample preparation. Bias voltages between –1.0 V and –1.2 V and current setpoints between 5 pA and 30 pA were applied to image the molecular adlayers shown in this work.

Mechanically cut Pt/Ir (80/20) tips were used and further modified *in situ* by applying short voltage pulses.

All STM images were *in situ* calibrated by subsequent immediate acquisition of an additional image at reduced bias voltage, therefore the atomic lattice of the HOPG surface is visible, which is used as a calibration grid. Data processing, also for image calibration, was performed using the SPIP 5 (Image Metrology) software package.

### 1.3 Transmission electron microscopy

Transmission electron microscopy (TEM) measurements were conducted on a FEI-Philips CM300 UT/FEG operated at 300 keV, equipped with a 2k $\times$ 2k CCD (Gatan MSC), an imaging filter (Gatan-GIF200), and an EDS system (Ge-detector, Thermo NSS6). The samples were prepared by wetting a holey carbon substrate with a 1 wt-% cyclohexane (CHX) gel of **1** as well as an in CHX diluted sample of the same gel. The samples were dried in air before measurements.

### 1.4 UV/vis spectroscopy

Temperature dependent UV/vis absorption measurements were conducted on a SPECORD 200 spectrometer (Analytic Jena) with a temperature controlled cuvette changer. The cuvette holder was heated and cooled by a water thermostat. The samples (solutions of **1-3** in methylcyclohexane (MCH)) were stored for at least one hour at 5 °C before starting the experiments. The deaggregation

was monitored by heating the cold samples stepwise from low temperatures (8–16 °C) to 40–60 °C. The samples were allowed to equilibrate by waiting 2–30 min at each temperature step. Equilibration was assumed when two consecutive measurements showed identical spectra.

## 1.5 Differential scanning calorimetry

Differential scanning calorimetry (DSC) measurements were performed on a METTLER TOLEDO DSC 823<sup>e</sup> with a HSS7-sensor and liquid nitrogen cooling. For the investigation of the gel samples, high pressure stainless steel crucibles with gold plated copper seals (METTLER TOLEDO) were used to prevent the evaporation of solvent.

The gels were prepared directly inside the crucibles. The substance was weighed into the crucible, CHX was added with an Eppendorf micropipette, and the crucible was then sealed instantly. The exact volume of cyclohexane was determined by weighing the whole crucible.

On all samples at least three heating and cooling cycles were performed to ensure reproducible results. The following heating and cooling methods were used:

**1<sup>st</sup> scan:** (after insertion) 1 min at 20°C, heating to 80°C with 5 K min<sup>-1</sup>, annealing at 80°C for 5 min, cooling to 10°C with –5 K min<sup>-1</sup> (Figure S1 A)

**2<sup>nd</sup> and 3<sup>d</sup> scan:** 30 min at 10°C, heating to 80°C with 5 K min<sup>-1</sup>, annealing at 80°C for 2 min, cooling to 10°C with –5 K min<sup>-1</sup> (Figure S1 B)

The second and third scan were started instantly after the previous scan. In Figure 2 (main text), the cooling curve of the 1<sup>st</sup> scan and the heating curve of the 2<sup>nd</sup> scan of the respective sample are depicted.

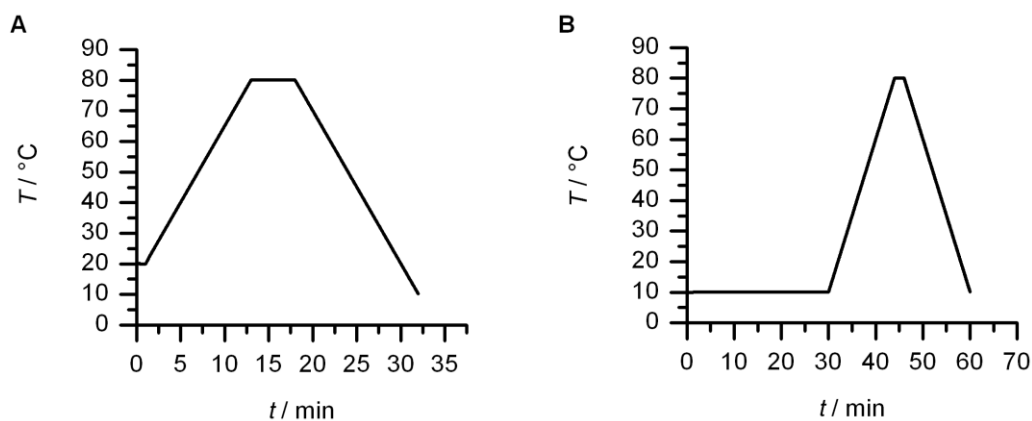


**Figure S1:** Temperature profile ( $T$  vs  $t$ ) of the two different measurement protocols (A: 1<sup>st</sup> scan, B: 2<sup>nd</sup> and 3<sup>rd</sup> scans).

## **1.6 Polarized optical microscopy**

Polarized optical microscopy (POM) was performed on a Leica DMLB microscope. Images were acquired with a Canimpex digital camera connected to a PC. Small pieces of the gels were put onto a glass slide and covered with a cover slip to reduce the evaporation of the solvent.

## 2 Molecular models

Molecular models of macrocycles **1-3** including side views and models of reference compounds are depicted in Figure S2.

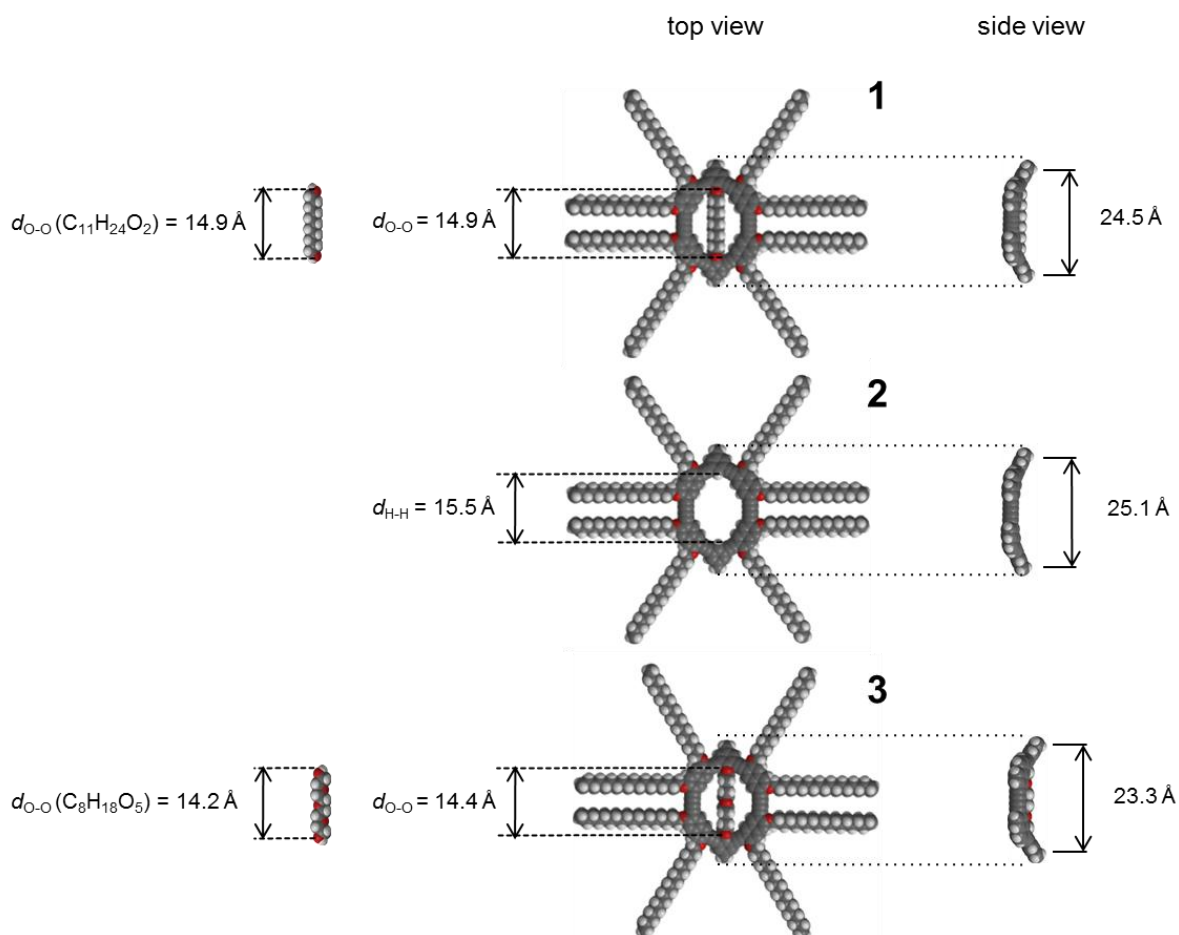


**Figure S2.** Molecular models of the macrocycles **1-3** are shown. Shape-persistent backbone structures of the macrocycles (with the respective interior strands for **1** and **3**) were derived by force-field calculation (Spartan '08), and extraannular all-trans configured octadecyloxy sidechains were subsequently added. The macrocycle dimensions are indicated (right part), and the cavity dimensions ( $d_{O-O}$ ) for **1** and **3** are referenced to the indicated O-O distances of (unstrained) 1,11-undecanediol, tetraethylene glycol, and  $d_{H-H}$  for **2**. The slightly varying macrocycle dimensions are induced by the intraannular strand.

### 3 Atomic force microscopy

#### 3.1 AFM images obtained from the gels

AFM images (and topography cross sections) of aggregates deposited from the gels of **1** (1 wt-%,  $2.5 \times 10^{-3}$  M, CHX) are shown in Figure S3a–i. The spinning procedure (cf. p. 4) leads to incomplete spreading of the gel material on the mica substrate. On top of the thick, dried, optically well visible material film densely packed fiber-shaped aggregates of **1** could be distinguished (Figure S3a, b, and h). Beside the edge of this bulk material, individual strands with lengths of a few  $\mu\text{m}$  are observed (Figure S3d–g, lower part in h). Height measurements, using the mica substrate as reference, indicate ribbon-shaped aggregates with widths in the order of 100 nm, which are as thin as  $4 \pm 0.5$  nm (see Main Text, Figures S3i and S4). Thicker aggregates were attributed to multiple layers of ribbon-like aggregates.

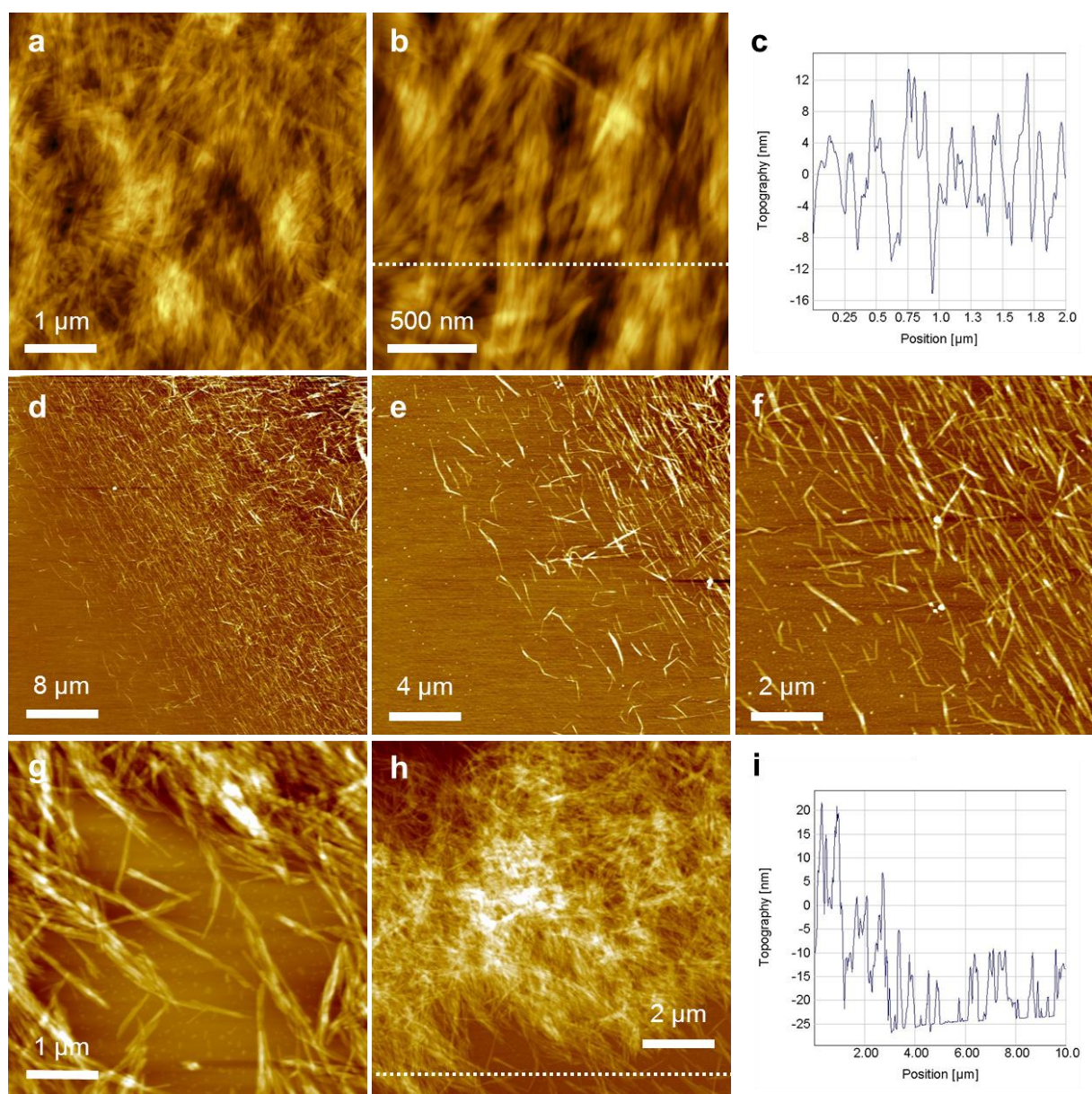


**Figure S3:** AFM images of aggregates of a CHX gel of **1** (1 wt-%,  $2.5 \times 10^{-3}$  M) after partly spreading the substance onto mica by spinning. (a) and (b) are obtained at the center of the sample, depicting the dried gel bulk. (c) shows a topography cross section along the dotted line in (b). (d)–(h) are obtained near/beside the edge of the gel material, and individual ribbons of a few  $\mu\text{m}$  length, supported on mica, can be clearly distinguished. The ribbons visible in (d)–(f) are oriented in parallel, as a result of the spinning procedure. (i) shows a topography cross section along the dotted line in (h), a reprint of Figure 2a (Main Text), giving an insight into the aggregate (and bundle) thickness distribution.

Larger images of CHX gel-cast aggregates of **1** (1 wt-%,  $2.5 \times 10^{-3}$  M) are shown in Figure S4. A doubled height (of  $7.5 \pm 0.5$  nm, line 2) is observed at the crossing point of two individual anisotropic aggregates (of diameters  $4.0 \pm 0.5$  nm, line 1, Figure S4).

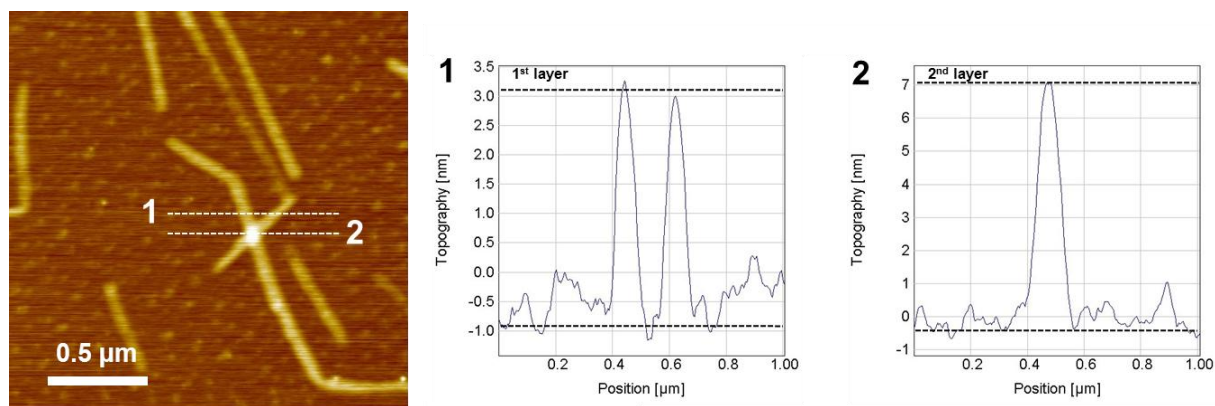


**Figure S4.** AFM image and topography cross sections of aggregates cast from a gel of **1** in CHX (1 wt-%,  $2.5 \times 10^{-3}$  M). Aside from ribbons, small spots are observed, attributed to smaller aggregates. The intermediate uncovered parts of the mica substrate are used as reference for the height measurements.

In an AFM scratching experiment, an individual line-scan was performed in contact mode, before and after imaging the sample (without changing the position) in tapping mode (Figure S5). At the line where the AFM tip was drawn (in contact) across the substrate, the aggregate structures are destroyed, and the molecules are “wiped away”. The result demonstrates the soft nature of the ribbons.

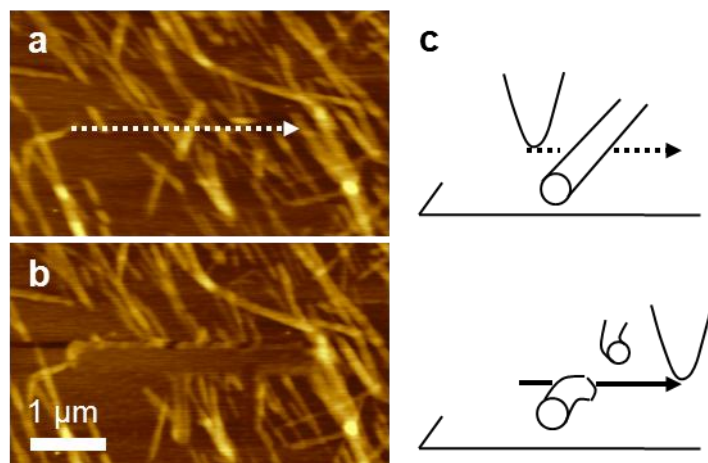


**Figure S5.** (a) and (b) Tapping-mode AFM images of aggregates of **1** cast from a gel (1 wt-%,  $2.5 \times 10^{-3}$  M, CHX) onto mica, before and after performing a line-scan (“scratch”) in contact-mode along the dotted arrow in (a). The scratching procedure is schematically shown in (c).

AFM images of aggregates deposited from the gels of **2** and **3** in cyclohexane (1 wt-%) are shown in Figures S6 and S7, respectively. The results are similar to the experiments performed for gels of **1**. For both compounds, ribbon-shaped aggregates are observed. The surface coverage varies here due to slightly varying gel casting conditions.

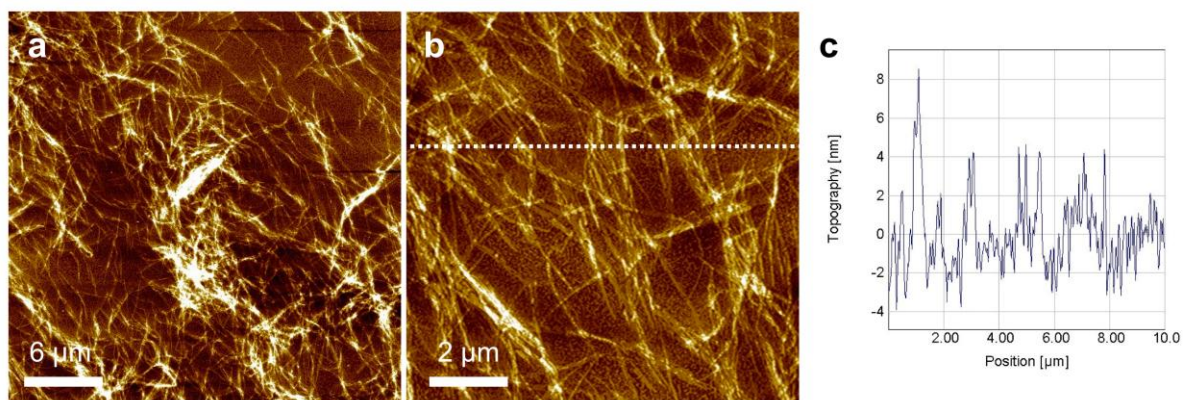


**Figure S6:** AFM images of a CHX-gel of **2** (1 wt-%,  $2.6 \times 10^{-3}$  M) on mica. (a)–(b) Fiber network and small dot-shaped aggregates on mica. (c) Topography cross section along the dotted line in (b).

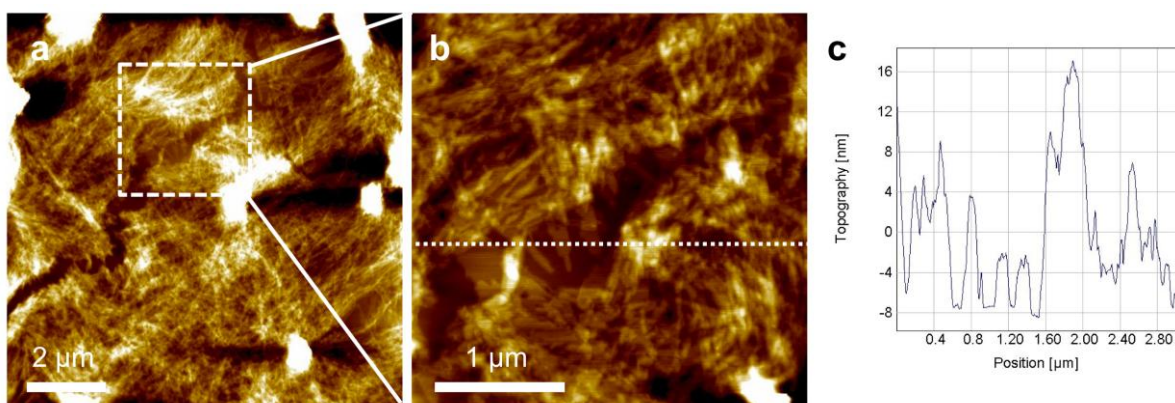


**Figure S7:** AFM images of a CHX-gel of **3** (1 wt-%,  $2.5 \times 10^{-3}$  M) on mica. (a) Bulk gel sample. The mica substrate is visible between the crack going from the lower left part to the upper right part of the image. (b) Detail image of the crack, where individual fibers point out onto the mica substrate. (c) Topography cross section along the dotted line in (b).

### 3.2 AFM images of aggregates cast from solution

Beside the option to image aggregates cast from a gel phase onto solid substrates, which requires sufficient spreading of the latter and/or imaging at the outer edge of the bulk gel material, ribbon like aggregates can be also deposited from diluted solutions. Figure S8a-b shows AFM images of aggregates dip-cast from a  $1.5 \times 10^{-4}$  M solution of **1** in MCH onto mica after storing the sample at 5 °C for 30 min. Compared to the aggregates found in the gel phase (of a few  $\mu\text{m}$  length, cf. Figures S3 and S4), several ten  $\mu\text{m}$  long strands were observed.

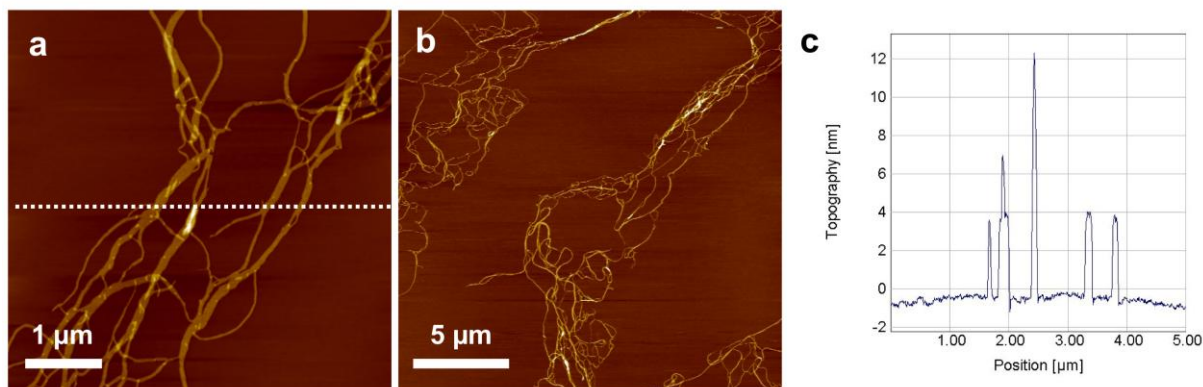


**Figure S8:** (a), (b) AFM images of aggregates of **1** formed in MCH (5 °C, 0.06 wt-%,  $1.5 \times 10^{-4}$  M); (c) topography cross-section along the dotted line in (a).

Ribbons of variable widths and uniform height of  $4.0 \pm 0.5$  nm are observed. The heights summate upon multilayer formation, caused by fiber crossing (Figure S9).

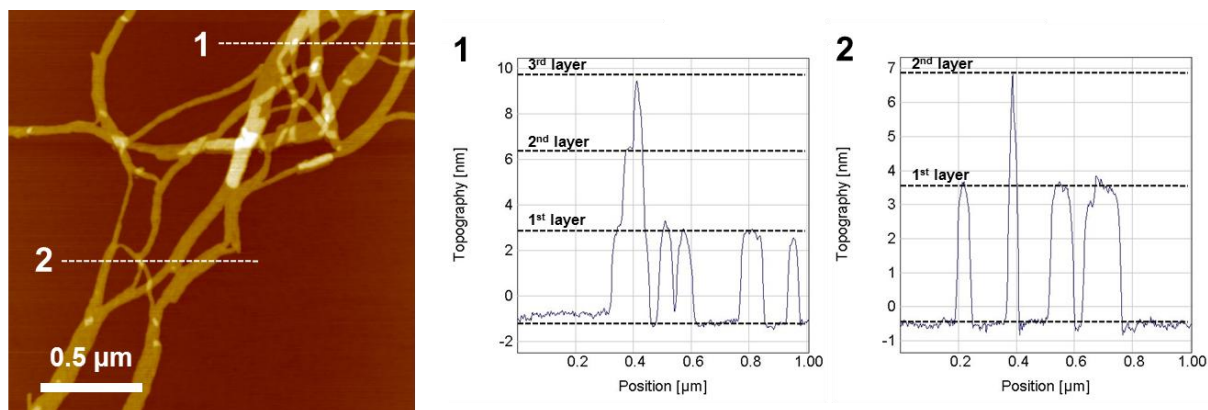


**Figure S9:** AFM image and topography cross sections of ribbons formed in MCH (5 °C,  $1.5 \times 10^{-4}$  M, 0.06 wt-%).

The results are significantly different from the observation after performing the similar experiment for solutions kept at 50 °C for 10 minutes (Figure S10), where only a film of 4 nm thickness (dewetting the substrate) and about 10-50 nm thick dots were observed (bright spots in Figure S10a-b). The absence of ribbon-like aggregates is consistent with the results observed by UV/vis measurements at elevated temperature (cf. p. S23).

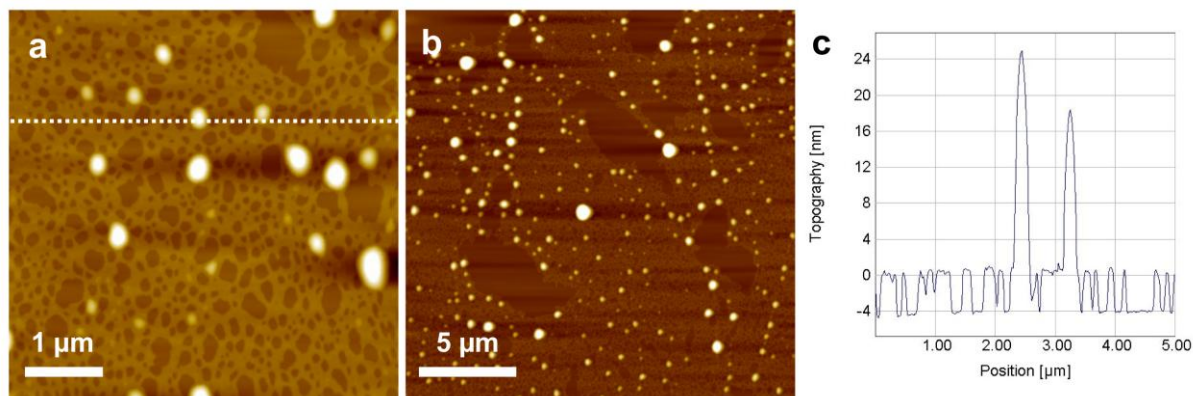


**Figure S10:** (a), (b) AFM topography images of the residue of an MCH solution of **1** ( $1.5 \times 10^{-4}$  M, 0.06 wt-%) dip cast at 50 °C; (c) topography cross-section along the dotted line in (a).

## **4 Transmission electron microscopy**

The transmission electron microscopy (TEM) images confirm the AFM results. Small ribbons with a diameter of 50 nm, which bundle to larger filaments of micrometer lengths and widths of around 150 to 250 nm, are observed (Figure S15).

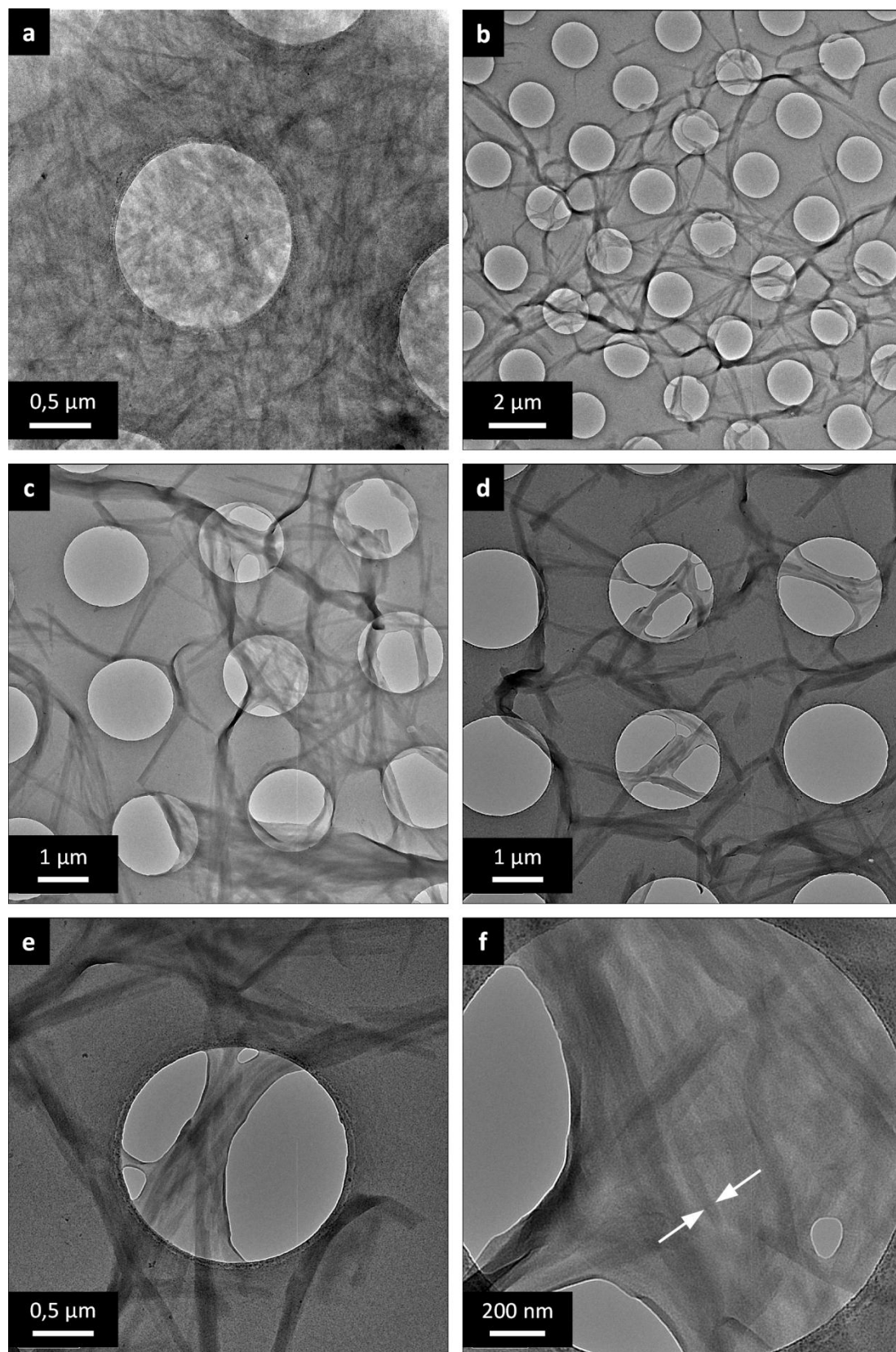


**Figure S15:** TEM micrographs of a dried gel sample of **1** in CHX on holey carbon. (a) Undiluted gel sample of 1 wt-%. A narrow web of one-dimensional aggregates is observed. (b)–(f) Diluted gel sample (CHX) at different magnifications; (f) the thinnest resolvable individual ribbons have a diameter of 50 nm (exemplarily marked by the two arrows).

## 5 UV/vis spectroscopy

Beside the deaggregation, side processes occurred (condensation of water at low  $T$ , precipitation), which disallowed the quantitative evaluation of the data. However, the spectra of all of the three samples show a blue-shift upon heating (i.e. deaggregation). The different spectra of the aggregated state and the solution state are presented in Figure S16.

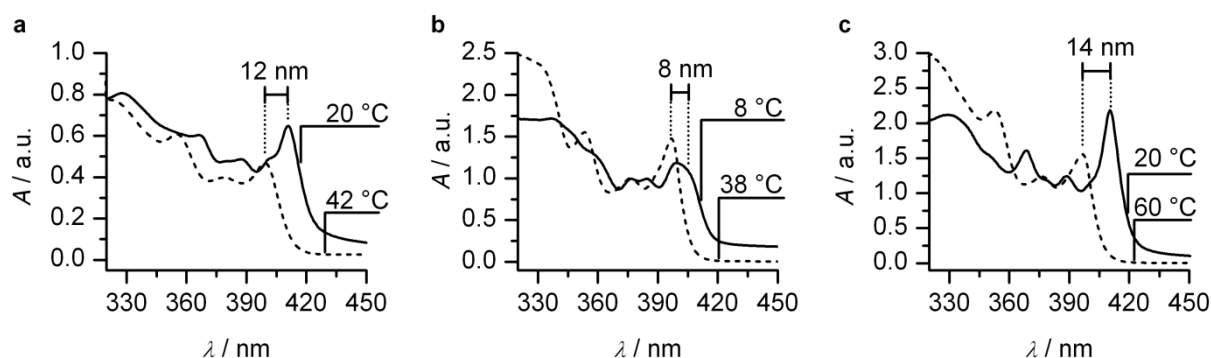


**Figure S16:** UV/vis spectra of MCH-solutions of **1** (a),  $c = 1.56 \times 10^{-4}$  M, 0.064 wt-%), **2** (b),  $c = 1.12 \times 10^{-4}$  M, 0.047 wt-%), and **3** (c),  $c = 3.92 \times 10^{-5}$  M, 0.016 wt-%) at low temperatures (—) and at elevated temperatures (---) after slow gradually heating.

Furthermore, the high-temperature spectrum of **3** in MCH ( $3.92 \times 10^{-5}$  M) and the absorption spectrum of **3** in  $\text{CHCl}_3$  ( $1.8 \times 10^{-4}$  M) at room temperature are nearly identical (Figure S17a). NMR (p. S50) has shown that in  $\text{CHCl}_3$  **3** is—even at a concentration of  $4.7 \times 10^{-3}$  M—molecularly dissolved. Because the mentioned spectra do not show significant differences, we conclude that at elevated temperatures the compounds in MCH are also completely dissolved. This was also confirmed by AFM (cf. p. S14). Additionally, varying the temperature of the  $\text{CHCl}_3$ -sample of **3** did not yield in varying spectra (Figure S17b). This means, this compound does not show thermochromism. Thus, the observed shifts in the spectra of the MCH-samples are solely caused by the aggregation process.

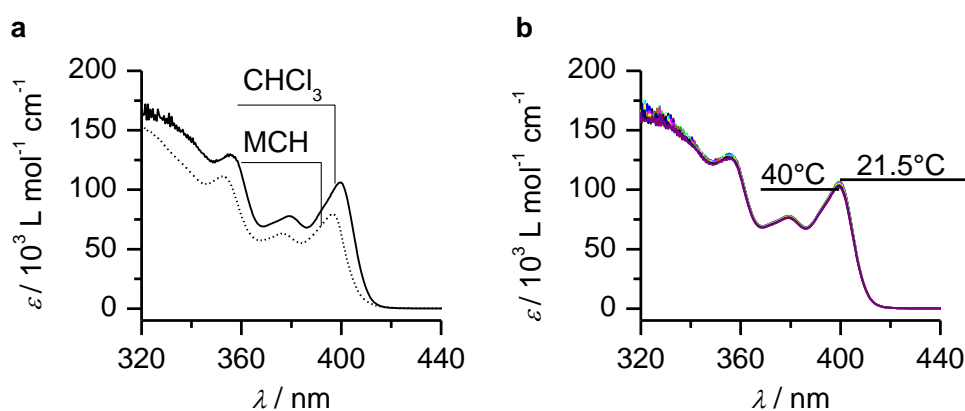


**Figure S17:** (a) Comparison of the UV/vis spectra of **3** in  $\text{CHCl}_3$  ( $c = 1.8 \times 10^{-4}$  M, —) and in MCH ( $c = 3.92 \times 10^{-5}$  M, .....). The spectra are almost identical. (b) UV/vis spectra of **3** in  $\text{CHCl}_3$  ( $c = 1.8 \times 10^{-4}$  M) at different temperatures.

## 6 Differential scanning calorimetry

Additional thermograms of DSC experiments on gel samples with varying concentrations are presented in Figure S18.

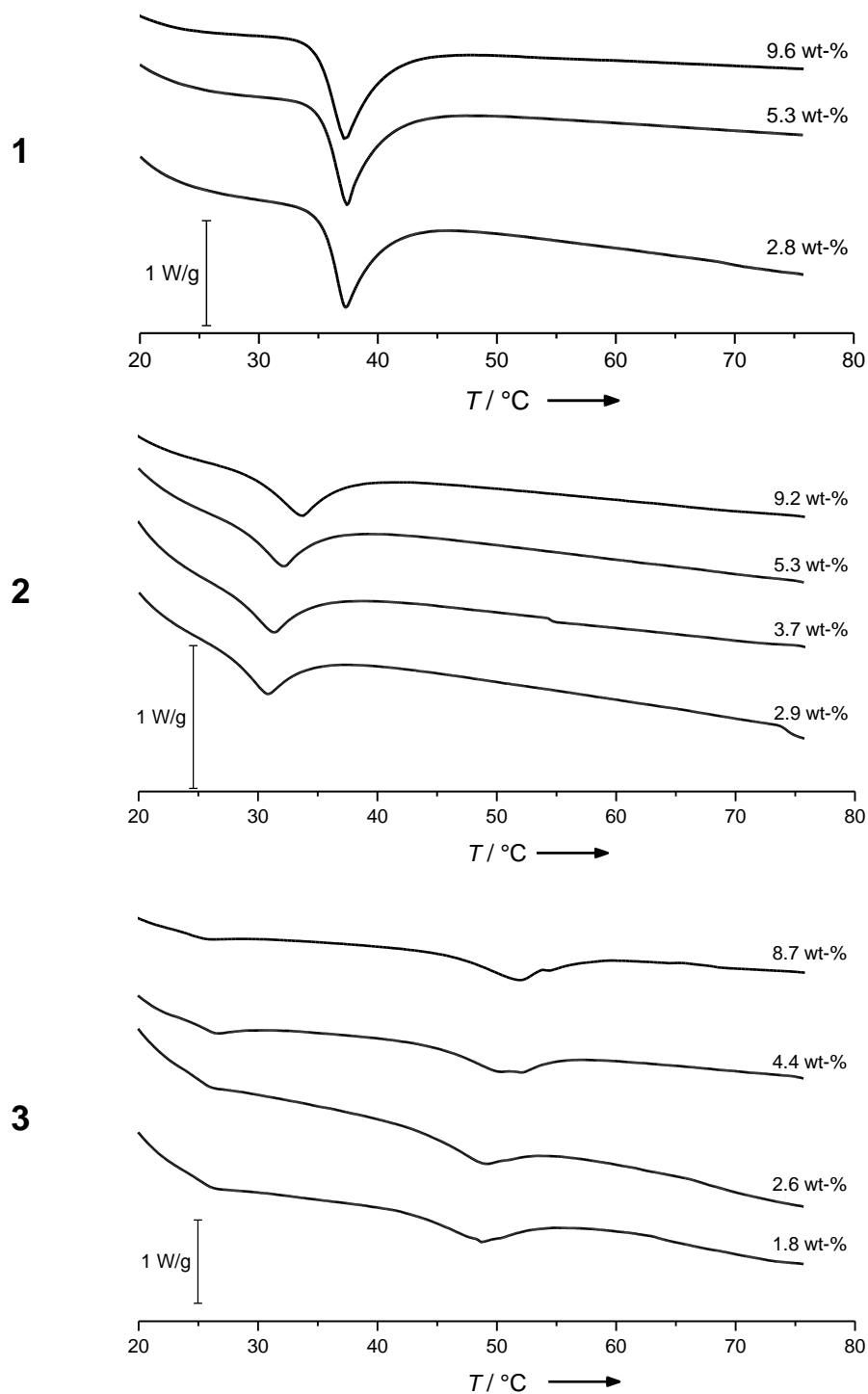


**Figure S18:** DSC heating scans of differently concentrated gels of **1**, **2**, and **3** in cyclohexane. The heat flow is scaled according to the amount of gelator.

## 7 Polarized optical microscopy

The inset in Figure S19a shows a POM image of a CHX-gel of **1** ( $c = 7.0 \times 10^{-3}$  M, 2.8 wt-%) directly after placing the sample onto the glass substrate. The bright texture indicates optical birefringence, which points on the existence of anisotropic aggregates (e. g. fibers or ribbons) in the gel state. After drying, a birefringent fibrous network becomes microscopically visible (Figure S19a), which is also resolvable in a (partly) dried gel sample of **2** in CHX ( $c = 7.7 \times 10^{-3}$  M, 2.9 wt-%, Figure S19b). These observations are consistent with the results of the AFM (cf. Figures S3, S4, S6) and TEM measurements (Figure S15).

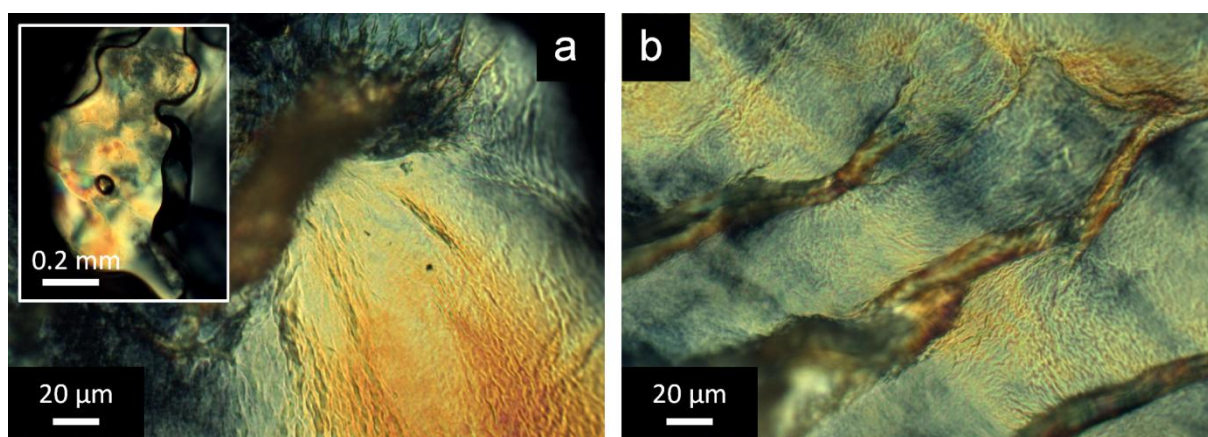


**Figure S19:** (a) POM image of a dried CHX-gel of **1** ( $c = 7.0 \times 10^{-3}$  M, 2.8 wt-%). The inset depicts the gel-sample directly after placing it onto the glass substrate. The black streak at the border of the colored area is the meniscus of the gel drop touching the cover slip. (b) Partially dried CHX-gel of **2** ( $c = 7.7 \times 10^{-3}$  M, 2.9 wt-%).

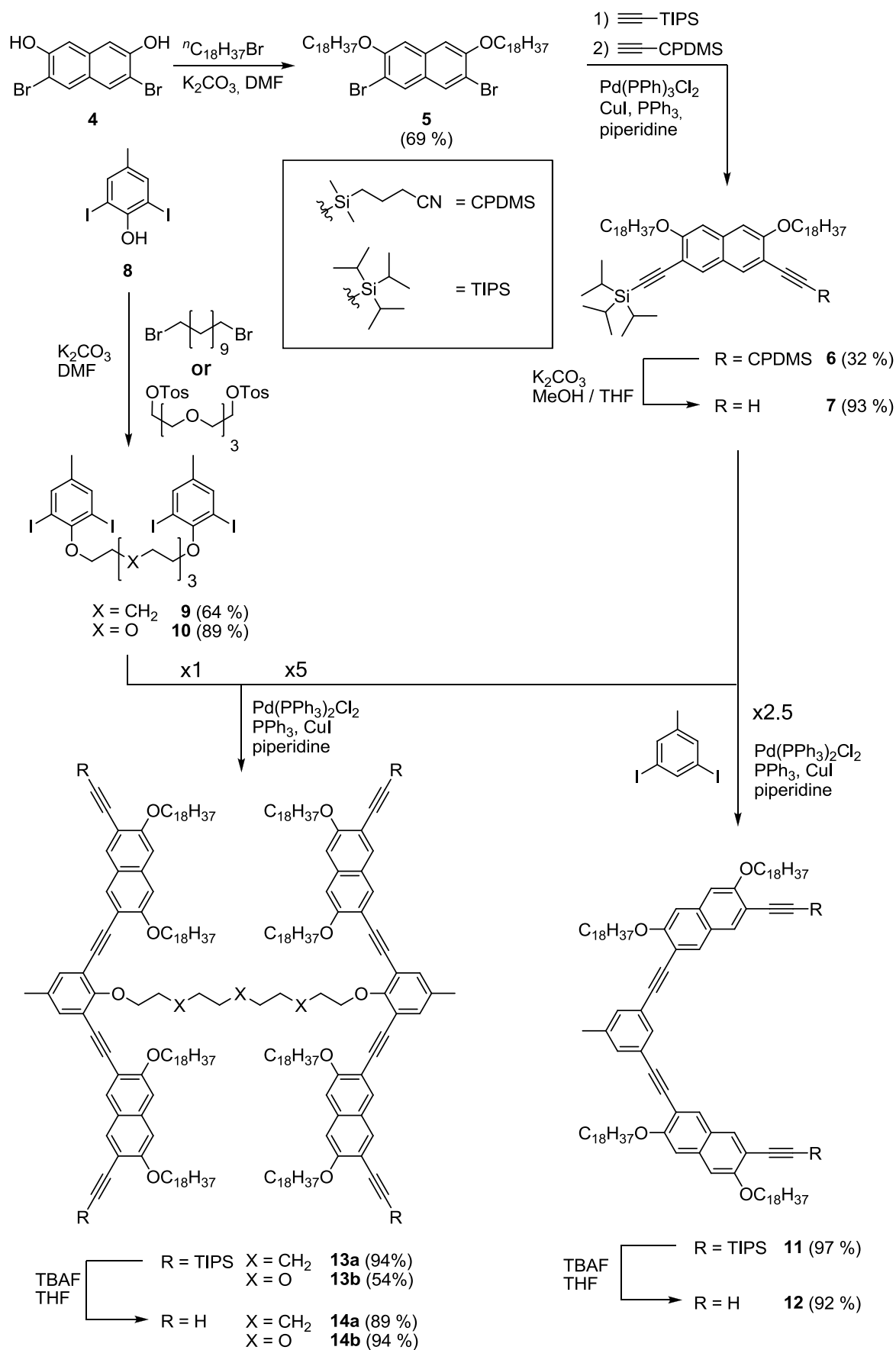
## 8 Synthesis

### 8.1 Overview

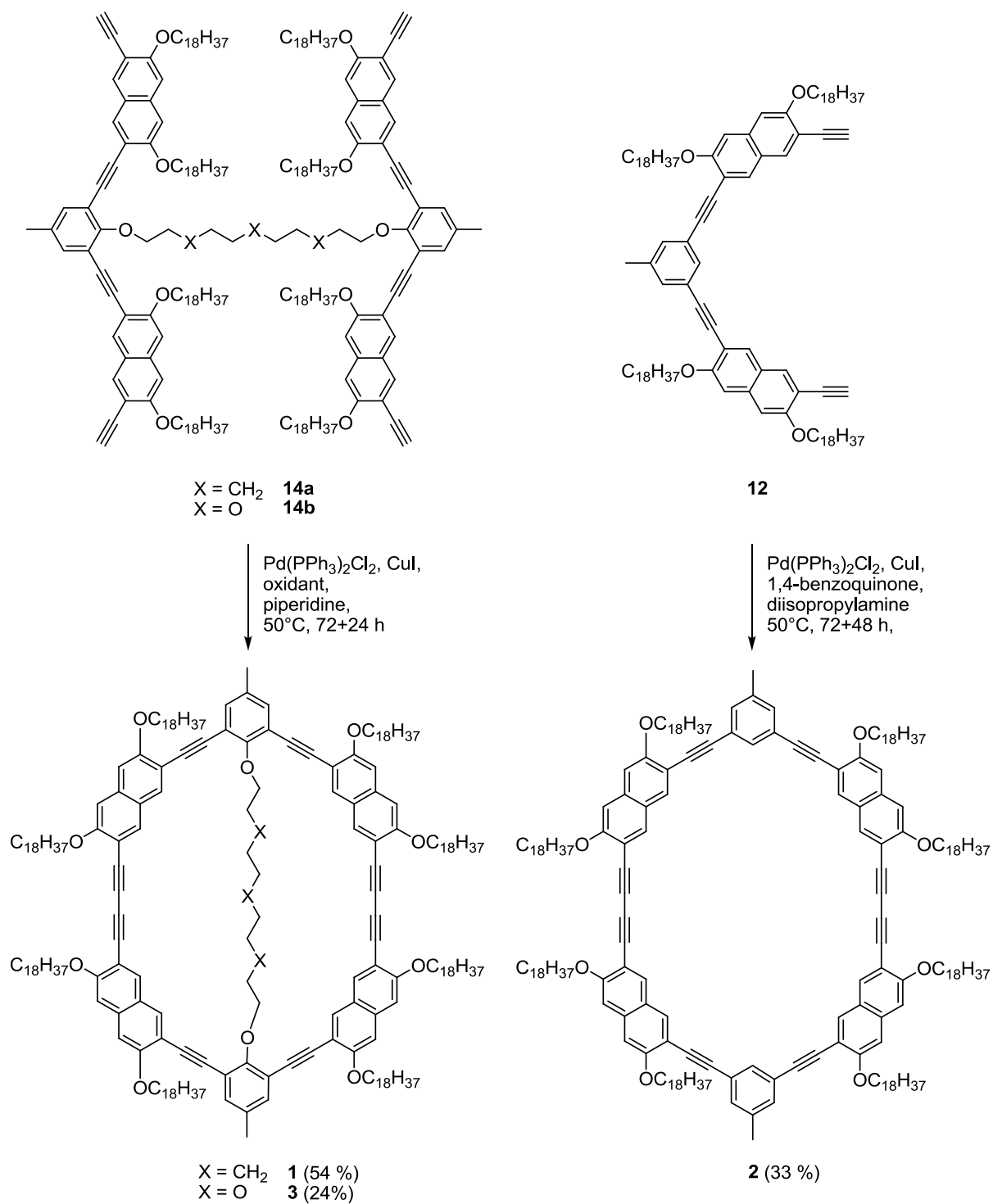
The synthesis of the macrocycles is based on a modular building block strategy. Considering macrocycles **1** and **3**, the target structures are composed of two building blocks: the naphthalene building block carrying the extraannular substituents and the template group carrying the intraannular moiety. After attaching the alkyl chains to 2,7-dibromo-3,6-dihydroxy naphthalene by a *Williamson* etherification,<sup>[4]</sup> the naphthalene derivative **5** is transformed into the unsymmetrical protected bisacetylene **6** following a statistical *Sonogashira-Hagihara* coupling protocol.<sup>[5]</sup> The selective removal of the labile (cyanopropyl)dimethylsilyl group (CPDMS) with potassium carbonate in methanol/THF yields the monoprotected bisacetylene **7**. The resulting acetylene is subsequently attached—again in a *Sonogashira-Hagihara* cross coupling reaction—to the respective template group (**9** or **10**). These template groups were synthesized by a two-fold *Williamson* etherification of either 1,11-dibromo undecane or tetra(ethylene glycol)di-*p*-tosylate and 2,6-diiodo-4-methylphenol (Scheme 1). Finally, after the removal of the TIPS protecting group with (tetra butyl)ammonium fluoride (TBAF), oxidative intramolecular dimerization of the terminal acetylene units by a palladium catalyzed *Glaser*-type coupling<sup>[6]</sup> under pseudo-high dilution conditions converts the precursors **14a,b** into the respective macrocycles **1** and **3** (Scheme 2).

The synthesis of the empty macrocycle **2** slightly varies from the aforementioned route. Instead of the template group, 3,5-diiodotoluene is coupled with the naphthalene derivative **7** to yield half-ring **11**. The subsequent steps are similar to the one described for **1** and **3**: deprotection yields the half-ring **12**, which is converted into macrocycle **2** using the same coupling protocol used for **1** and **3** (Scheme 1 and 2).

The GPC analysis of the cyclization products demonstrates that in the cyclization of **1** and **3** only traces of oligomers are formed (Figure 36, Figure 39) whereas in the dimerization of half-ring **12** the formation of larger amounts of oligomers is observed (Figure 46). This is attributed to the template effect, evoked by the covalent linkage of the half-rings.<sup>[7]</sup> Notably, the dimerization of **12** only leads to macrocycle formation if the described Pd-catalyst is used. By contrast, using CuCl/CuCl<sub>2</sub>/pyridine leads to polymerization of the precursor. A similar phenomenon was recently described for the cyclization of pyridine-containing macrocycles.<sup>[6b]</sup>

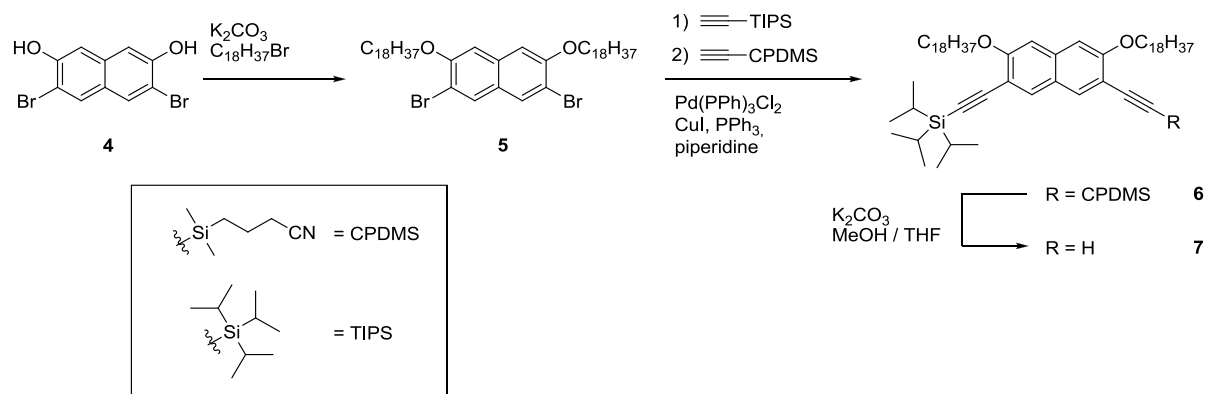


**Scheme S1.** Synthetic route to the tetraacetylenes **14a,b** and bisacetylene **12**.



**Scheme S2.** Cyclization of the respective precursors towards the macrocycles **1–3**. Oxidant: iodine (**1**) and 1,4-benzoquinone (**3**), respectively.

## 8.2 Synthesis and characterization of building blocks 7, 9, 10



**Scheme S3:** Reaction pathway towards building block 7.

**Synthesis of 2,7-dibromo-3,6-di(octadecoxy)naphthalene 5.** Under an argon atmosphere 2,7-dibromo-3,6-(dihydroxy)naphthalene **4** (1.00 g, 3.15 mmol),<sup>[1]</sup> 1-bromooctadecane (2.33 g, 6.99 mmol), anhydrous K<sub>2</sub>CO<sub>3</sub> (3.50 g, 25.00 mmol), and KI (12 mg, 72.2 μmol) were suspended in dry DMF (10 mL) and heated up to 60 °C. After stirring for 20 h the mixture was allowed to cool to room temperature and diluted with water. The residue was filtered and washed with water and methanol. After drying in vacuum, **5** was isolated as a white solid (1.78 g, 2.168 mmol, 69 %) and used as received. M.p. 80 °C. <sup>1</sup>H NMR (CDCl<sub>3</sub>, 400MHz): δ (ppm) = 7.86 (s, 2H, ArH), 6.99 (s, 2H, ArH), 4.09 (t, *J* = 6.49 Hz, 4H, OCH<sub>2</sub>), 1.90 (m, 4H, CH<sub>2</sub>), 1.54 (m, 4H), 1.45–1.81 (m, 48H), 0.88 (t, *J* = 6.86 Hz, 6H, CH<sub>3</sub>).

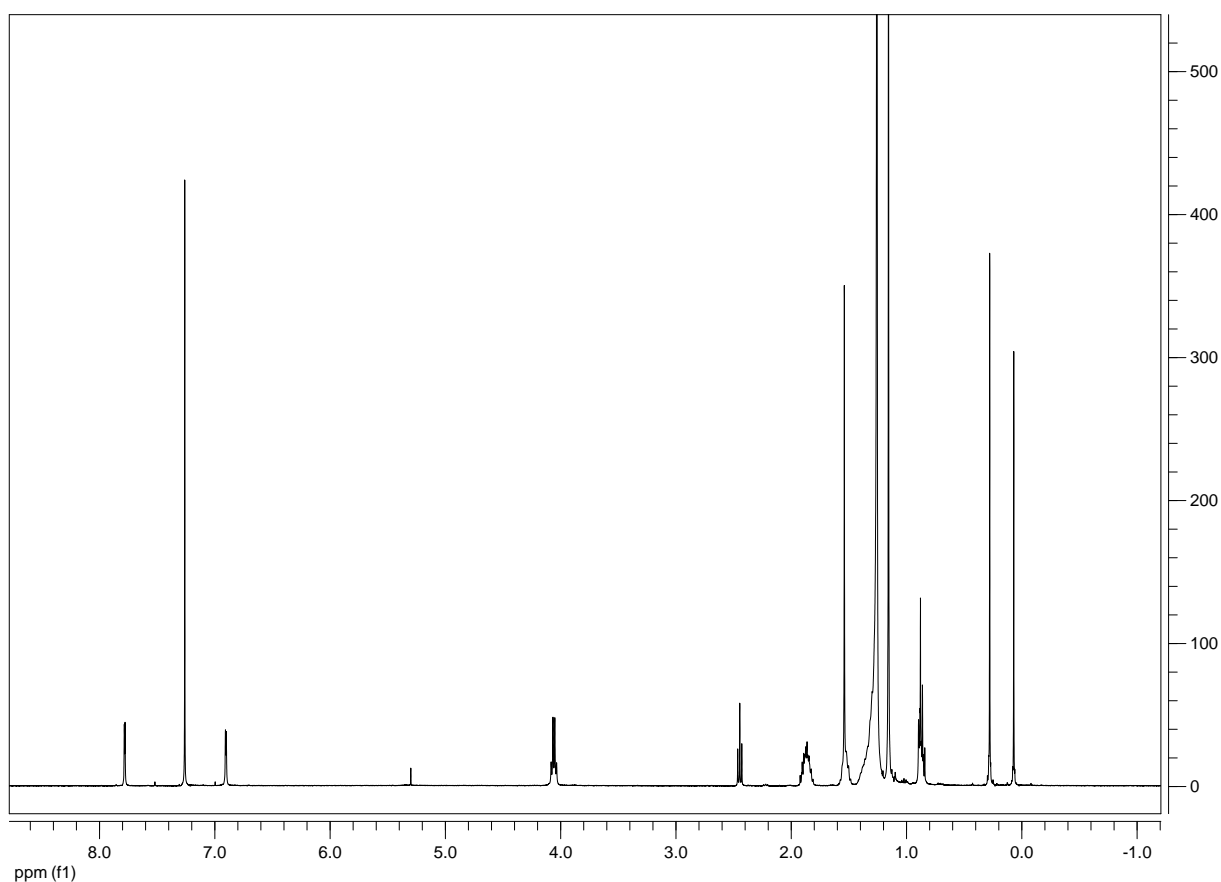


**Figure S20:** <sup>1</sup>H NMR (400 MHz, CDCl<sub>3</sub>) of **5**.

**Synthesis of 6.** **5** (1.23 g, 1.495 mmol), Pd(PPh<sub>3</sub>)Cl<sub>2</sub> (16 mg, 0.023 mmol), PPh<sub>3</sub> (16 mg, 0.061 mmol), and CuI (8 mg, 0.042 mmol) were dissolved in dry piperidine (5 mL) and heated to 60 °C. Triisopropylsilylacetylene (0.29 g, 1.590 mmol) was added and the mixture was stirred for 18 h. After adding CPDMS-acetylene<sup>[3]</sup> (0.45 g, 2.975 mmol) the reaction was stirred for additional 3 h before cooling down to room temperature. The reaction was diluted with CH<sub>2</sub>Cl<sub>2</sub>, and the organic layer was subsequently extracted with water (3x), aqueous acetic acid (10 %, v/v), aqueous NaOH (10 %), and brine. After drying over MgSO<sub>4</sub> the solvent was evaporated. The product was purified by column chromatography (silica gel, petroleum ether : CH<sub>2</sub>Cl<sub>2</sub> = 2 : 1, R<sub>f</sub> = 0.44) yielding **6** as a yellowish oil (0.470 g, 0.472 mmol, 32 %). <sup>1</sup>H NMR (300 MHz, CDCl<sub>3</sub>): δ [ppm] = 7.78 (s; 1H, ArH), 7.77 (s; 1H, ArH), 6.91 (s; 1H, ArH), 6.90 (s; 1H, ArH), 4.07 (t, J = 6.42 Hz, 2H, OCH<sub>2</sub>), 4.05 (t; 2H, J = 6.23 Hz, 2H, OCH<sub>2</sub>), 2.44 (t, J = 7.05 Hz, 2H, CH<sub>2</sub>-CN), 1.86 (m, 6H, OCH<sub>2</sub>CH<sub>2</sub>, CH<sub>2</sub>CH<sub>2</sub>CN), 1.55–1.20 (m, 60H), 1.15 (s, 21H, TIPS), 0.87 (m, 8H, SiCH<sub>2</sub>C<sub>2</sub>H<sub>4</sub>CN, OC<sub>17</sub>H<sub>34</sub>CH<sub>3</sub>), 0.27 (s, 6H, Si(CH<sub>3</sub>)<sub>2</sub>). MALDI-MS (DCTB): m/z = 993.8 (M<sup>+</sup>), C<sub>65</sub>H<sub>111</sub>NO<sub>2</sub>Si<sub>2</sub> requires 993.82.

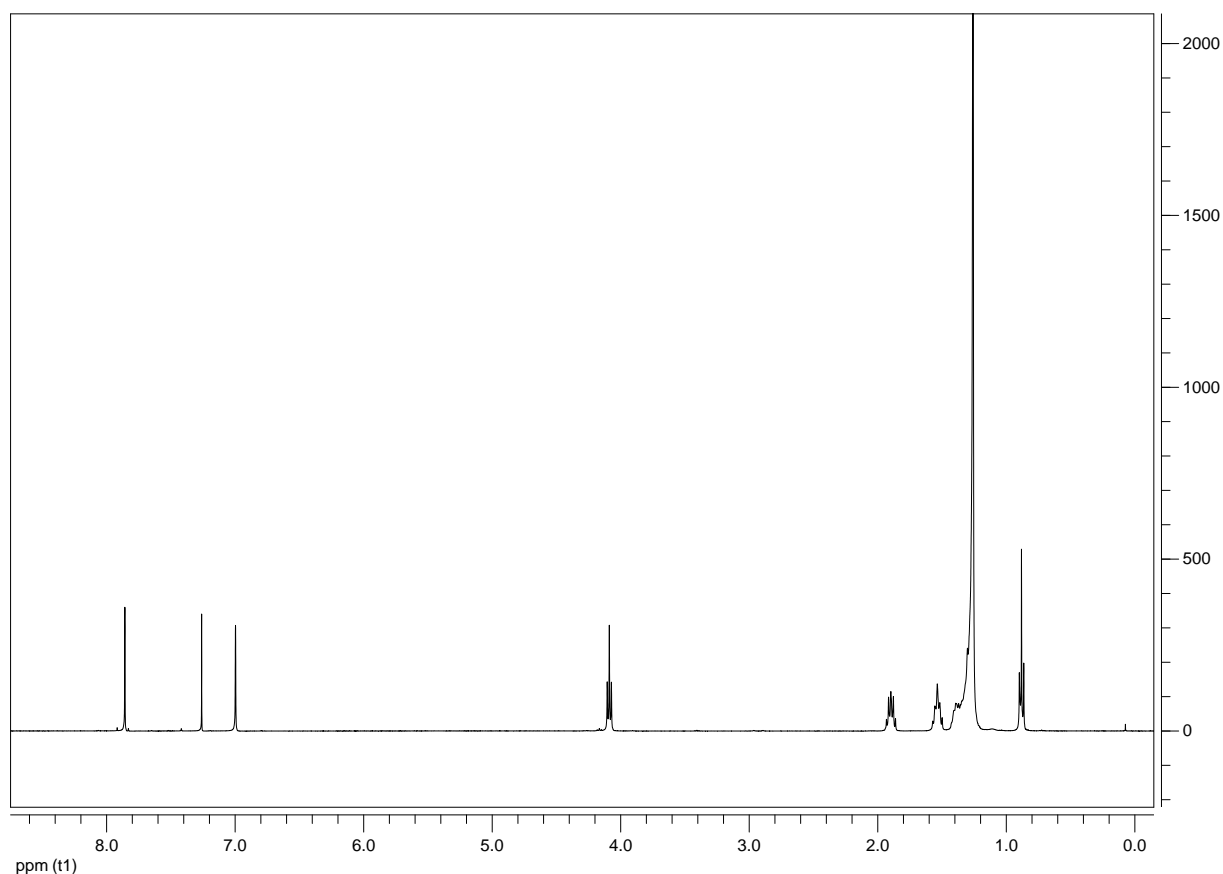


**Figure S21:** <sup>1</sup>H NMR (300 MHz, CDCl<sub>3</sub>) of **6**.

**Synthesis of 7.** To a solution of **6** (470 mg, 472  $\mu\text{mol}$ ) in THF (3 mL)  $\text{K}_2\text{CO}_3$  (180 mg, 1.420 mmol) and MeOH (3mL) were added. After stirring for 2 h the mixture was diluted with  $\text{CH}_2\text{Cl}_2$  and extracted with water (3x) and brine. The solvent was evaporated and the resulting yellow oil was purified by column chromatography (silica gel, petroleum ether :  $\text{CH}_2\text{Cl}_2$  = 3 : 1,  $R_f$  = 0.30) to obtain **7** (380 mg, 437  $\mu\text{mol}$ , 93 %) as a colorless solid. M.p. 60 °C.  $^1\text{H}$  NMR (400 MHz,  $\text{CDCl}_3$ ):  $\delta$  [ppm] = 7.82 (s, 1H, ArH), 7.80 (s, 1H, ArH), 6.94 (s, 1H, ArH), 6.91 (s, 1H, ArH), 4.10 (t,  $J$  = 6.6 Hz, 2H,  $\text{OCH}_2$ ), 4.06 (t,  $J$  = 6.3 Hz, 2H,  $\text{OCH}_2$ ), 3.25 (s, 1H, alkyne-H), 1.94–1.79 (m, 4H,  $\text{OCH}_2\text{CH}_2$ ), 1.60–1.46 (m, 4H), 1.45–1.20 (m; 56H), 1.15 (s, 21H, TIPS), 0.87 (t,  $J$  = 6.8 Hz, 6H,  $\text{OC}_{17}\text{H}_{34}\text{CH}_3$ ).  $^{13}\text{C}$  NMR (100 MHz,  $\text{CDCl}_3$ ):  $\delta$  [ppm] = 158.49, 158.01, 135.97, 134.18, 133.69, 122.70, 112.98, 111.22, 105.46, 105.09, 103.18, 94.70, 80.69, 80.29, 68.81, 68.63, 32.08, 29.86, 29.84, 29.82, 29.76, 29.74, 29.68, 29.52, 29.48, 29.13, 26.45, 26.16, 22.85, 18.89, 14.27, 11.58. MS (ESI, 10 eV):  $m/z$  = 891.7 ( $\text{M}+\text{Na}$ ) $^+$ , 869.8 ( $\text{M}+\text{H}$ ) $^+$ ,  $\text{C}_{59}\text{H}_{100}\text{O}_2\text{Si}$  requires 868.75.

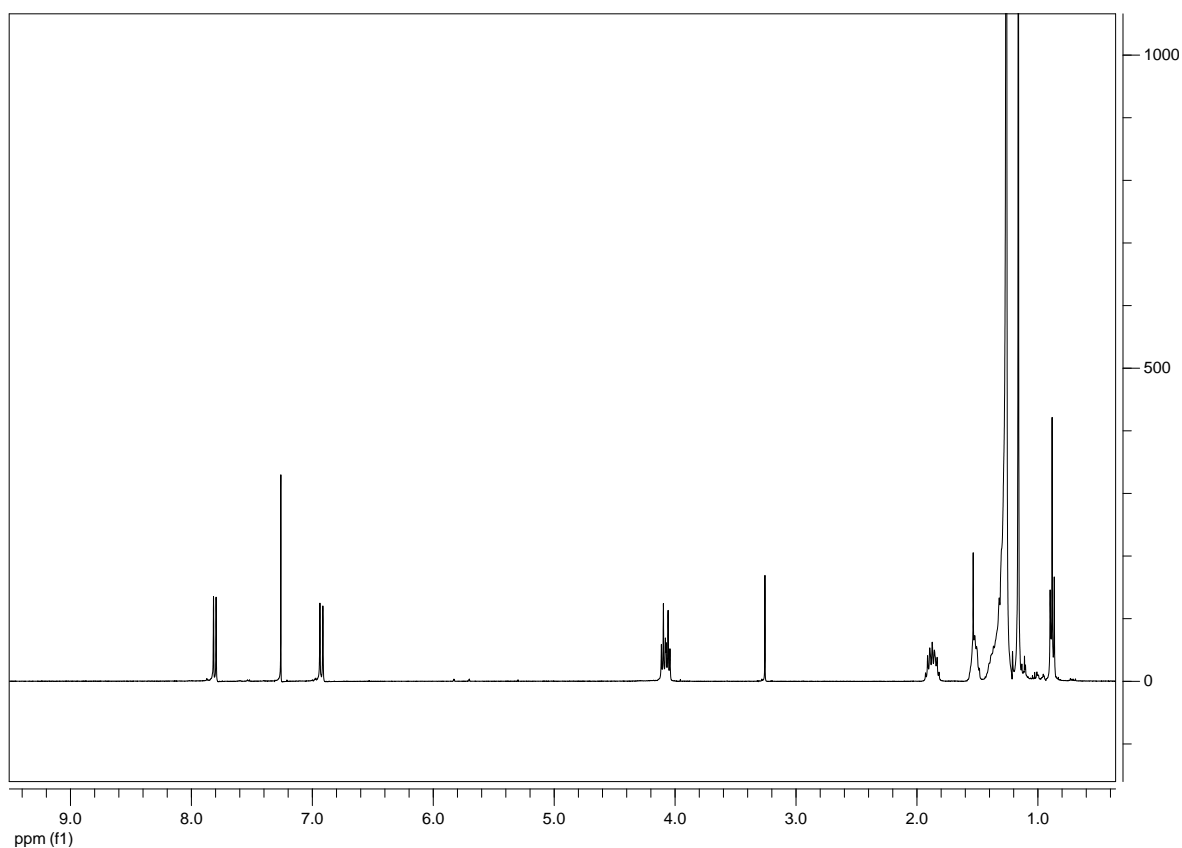


**Figure S22:**  $^1\text{H}$  NMR (400 MHz,  $\text{CDCl}_3$ ) of **7**.

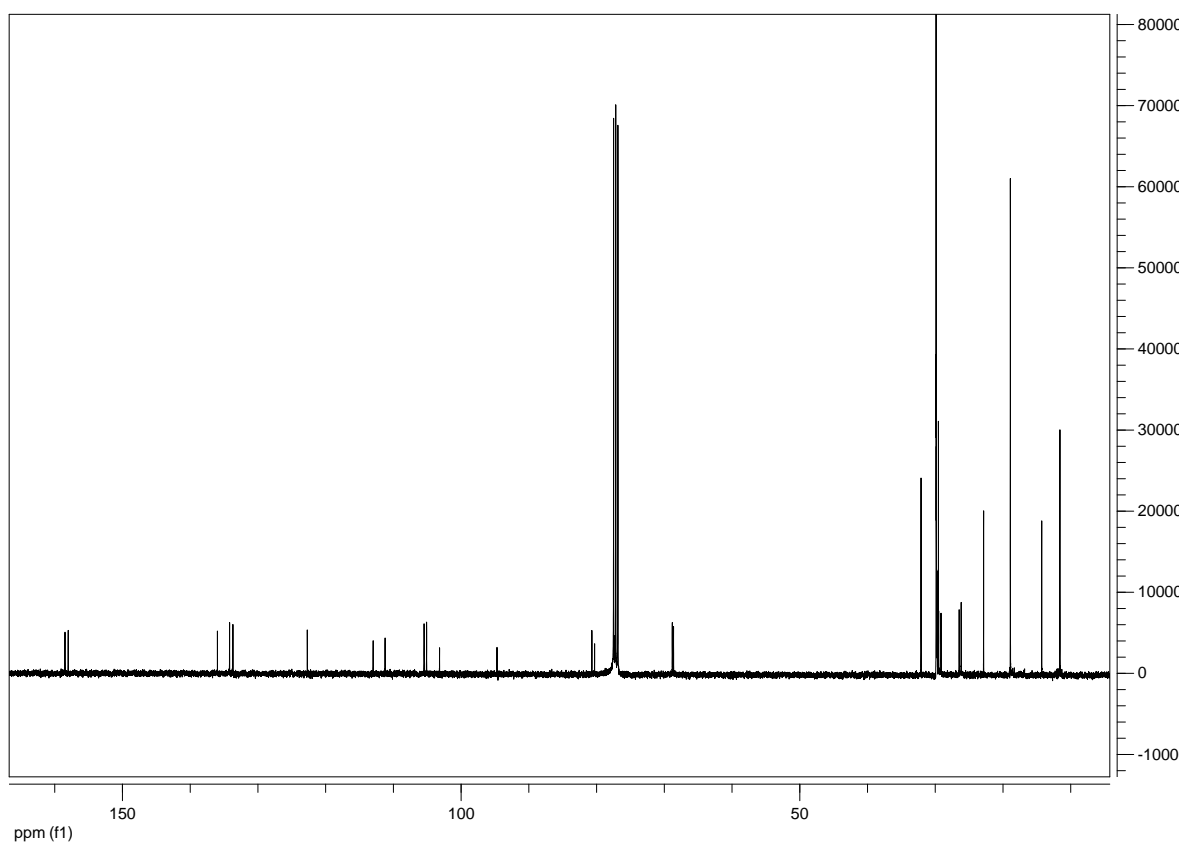
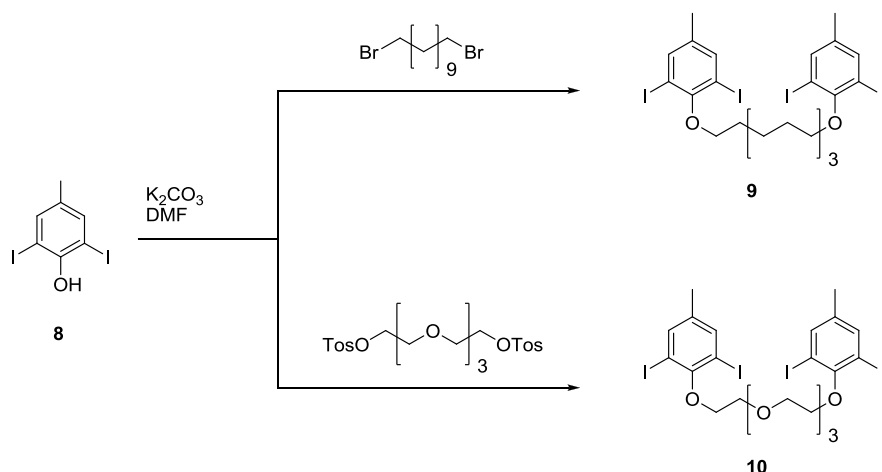


**Figure S23:**  $^{13}\text{C}$  NMR (100 MHz,  $\text{CDCl}_3$ ) of **7**.



**Scheme S4:** Reaction scheme towards the template strands **9** and **10**.

**Synthesis of 9.** 2,6-Diiodo-4-methylphenol **8**<sup>[8]</sup> (200 mg, 0.556 mmol) and 1,11-dibromoundecane (93 mg, 0.296 mmol) were dissolved in DMF (2 mL). After adding  $K_2CO_3$  (467 mg, 3.379 mmol) and KI (13 mg, 78.3  $\mu$ mol) the mixture was heated to 60 °C and stirred for 16 h. The reaction mixture was then cooled to room temperature and diluted with  $CH_2Cl_2$  and water. The organic layer was separated and subsequently extracted with water (3x), aqueous acetic acid (10 % v/v, 3x), water, aqueous NaOH (10 %, w/w), and brine. After drying ( $MgSO_4$ ), the solvent was removed under reduced pressure. The yellow residue was purified by column chromatography (silica gel, petroleum ether :  $CH_2Cl_2$  = 5 : 1,  $R_f$  = 0.36) to yield **9** (166 mg, 0.190 mmol, 64 %) as a colorless solid. M.p. 90–93 °C.  $^1H$  NMR (400 MHz,  $CDCl_3$ ):  $\delta$  [ppm] = 7.57 (d,  $J$  = 0.6 Hz, 2H, ArH), 3.93 (t,  $J$  = 6.6 Hz, 4H,  $OCH_2$ ), 2.22 (s, 1.87, 6H, Ar $CH_3$ ), 1.89 (m, 4H,  $OCH_2CH_2$ ), 1.61–1.29 (m; 14H).  $^{13}C$  NMR (100 MHz,  $CDCl_3$ ):  $\delta$  [ppm] = 155.78, 140.23, 137.44, 90.54, 73.43, 30.02, 29.57, 29.50, 25.97, 19.61. MS (ESI, 10 eV):  $m/z$  = 894.9 ( $M+Na$ )<sup>+</sup>,  $C_{25}H_{32}I_4O_2$  requires 871.86.

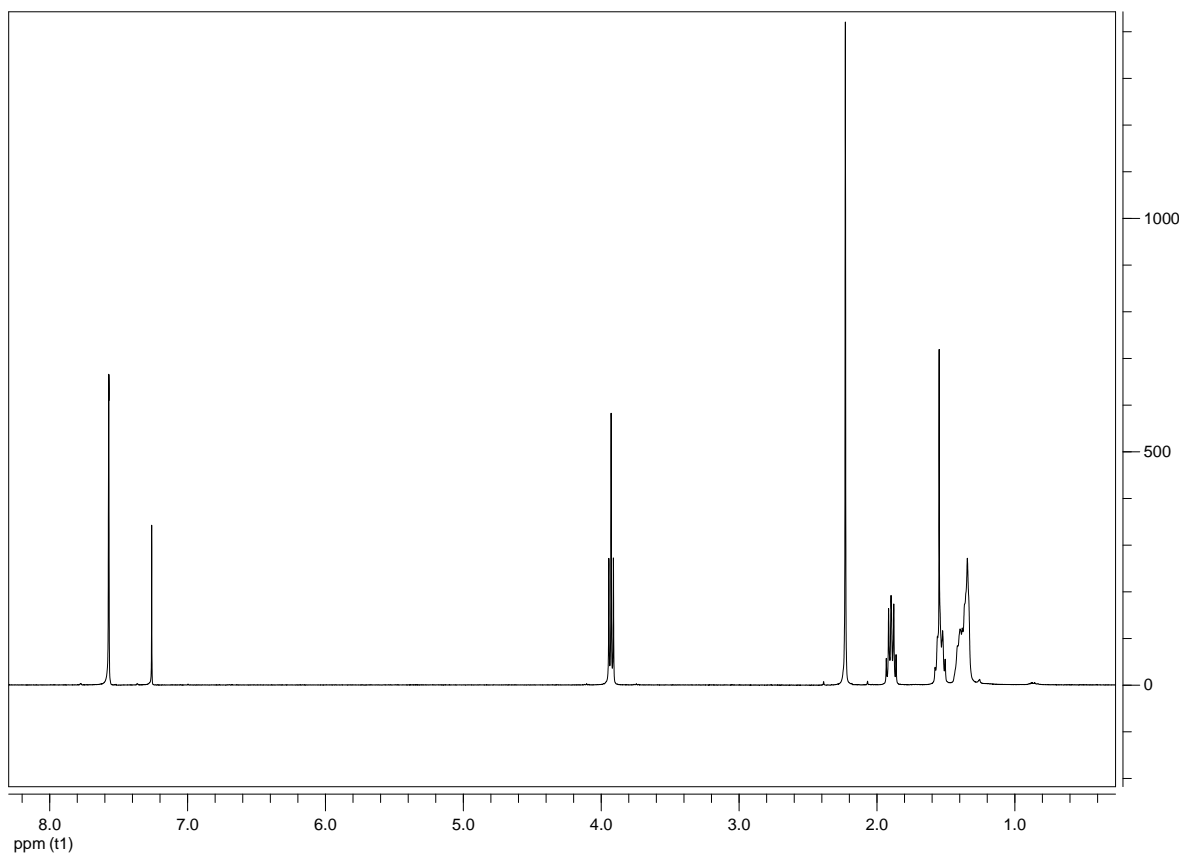


**Figure S24:** <sup>1</sup>H NMR (400 MHz, CDCl<sub>3</sub>) of **9**.

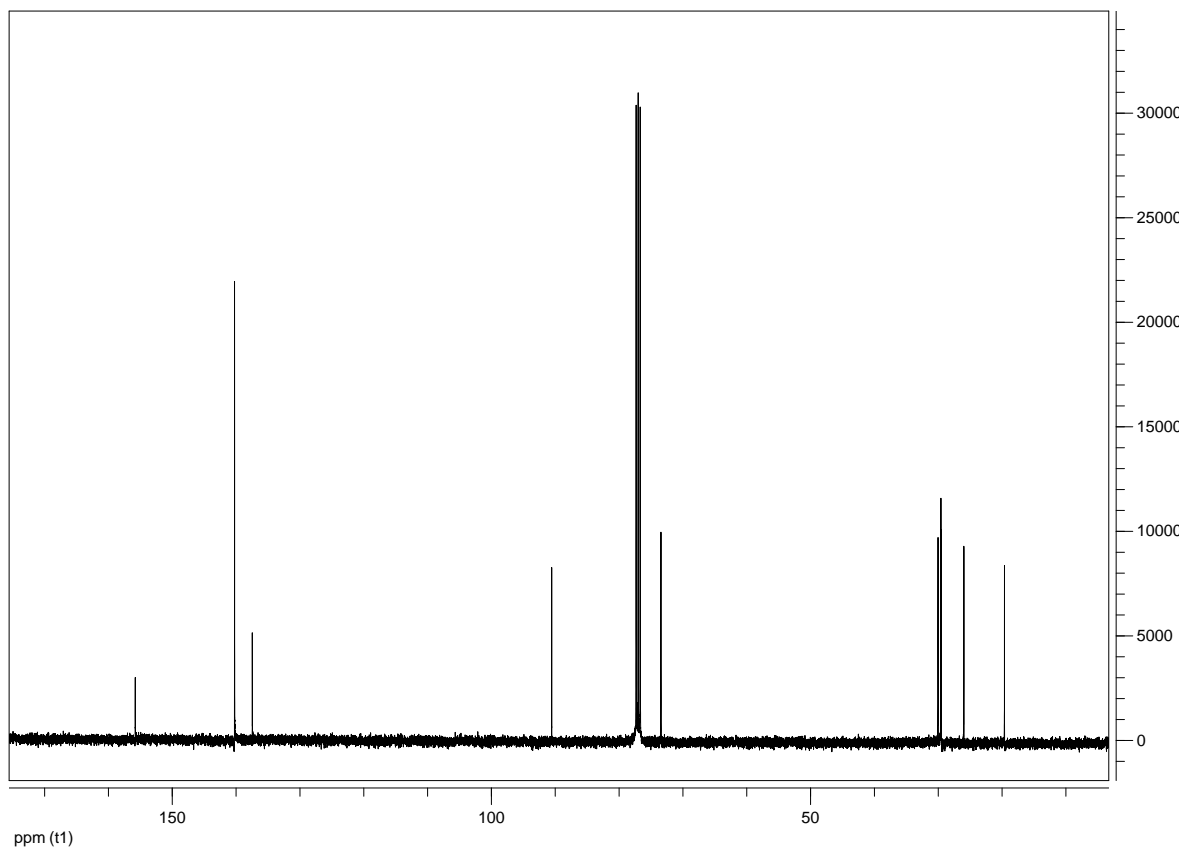


**Figure S25:** <sup>13</sup>C NMR (100 MHz, CDCl<sub>3</sub>) of **9**.

**Synthesis of 10.** To a solution of 2,6-diiodo-4-methylphenol **8** (1.48 g, 4.19 mmol) and tetra(ethylene glycol)di-*p*-tosylate (1.03 g, 2.05 mmol) in DMF (6 mL)  $K_2CO_3$  (1.71 g, 12.4 mmol) was added. The reaction mixture was stirred for 18 h at 60 °C. After cooling down to room temperature diethyl ether and water were added. The organic layer was extracted with water (3x) and brine and subsequently dried over  $MgSO_4$ . The solvent was evaporated, and the residue was purified by column chromatography (silica gel,  $CH_2Cl_2$  : MeOH = 100 : 1,  $R_f$  = 0.89). **10** is received as a colorless solid (1.60 g, 1.82 mmol, 89 %). M.p. 68–70 °C.  $^1H$  NMR (500 MHz,  $CDCl_3$ ):  $\delta$  [ppm] = 7.57 (d,  $J$  = 0.7 Hz, 2H, ArH), 4.12 (t,  $J$  = 5.1 Hz, 4H,  $ArOCH_2CH_2$ ), 3.97 (t,  $J$  = 5.1 Hz, 4H,  $ArOCH_2CH_2$ ), 3.85–3.78 (m, 4H,  $CH_2OCH_2CH_2OCH_2$ ), 3.78–3.71 (m, 4H,  $CH_2OCH_2CH_2OCH_2$ ), 2.23 (s, 6H,  $ArCH_3$ ).  $^{13}C$  NMR (125 MHz,  $CDCl_3$ ):  $\delta$  [ppm] = 155.45, 140.25, 137.70, 90.39, 72.13, 70.90, 70.81, 70.07, 19.62. MS (ESI, 10 eV):  $m/z$  = 900.8 ( $M+Na$ ) $^+$ , 878.8 ( $M+H$ ) $^+$ , 751.9 ( $M-I$ ) $^+$ ,  $C_{22}H_{26}I_4O_5$  requires 877.80.

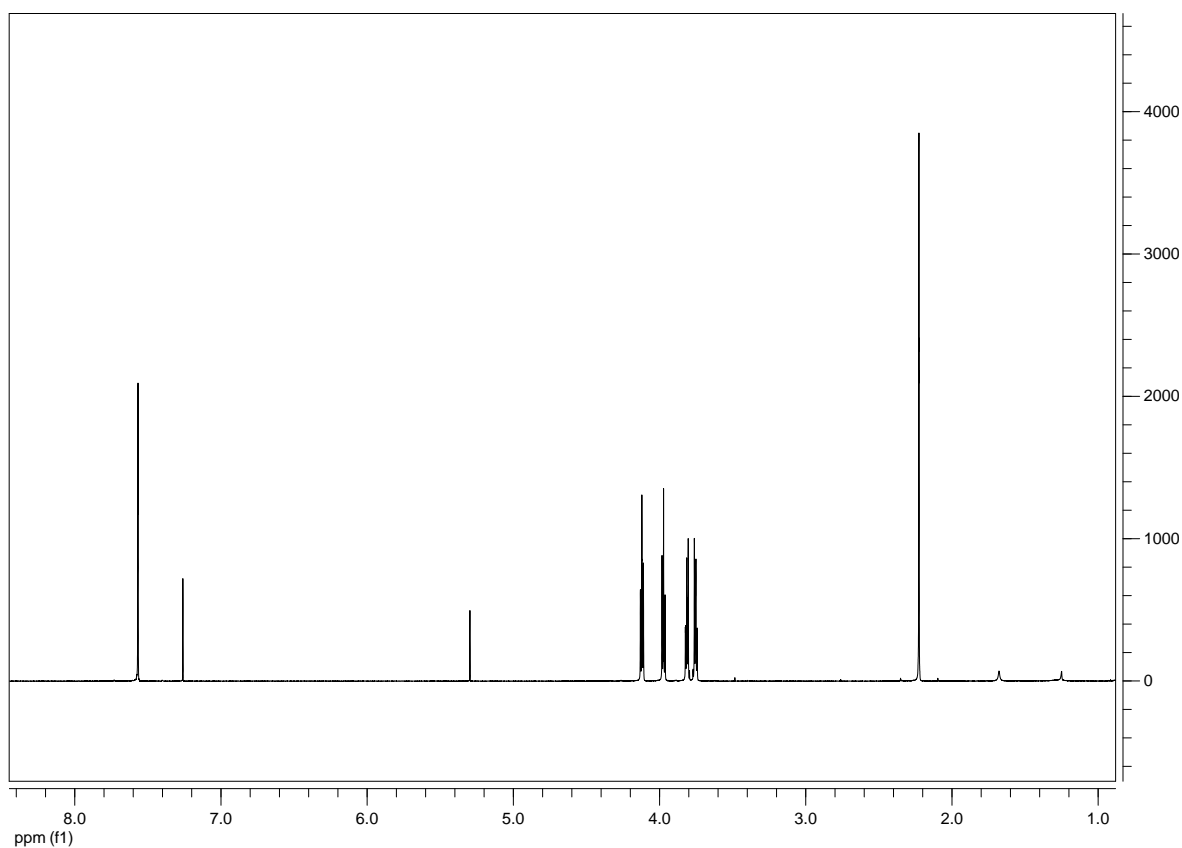


**Figure S26:**  $^1H$  NMR (500 MHz,  $CDCl_3$ ) of **10**.

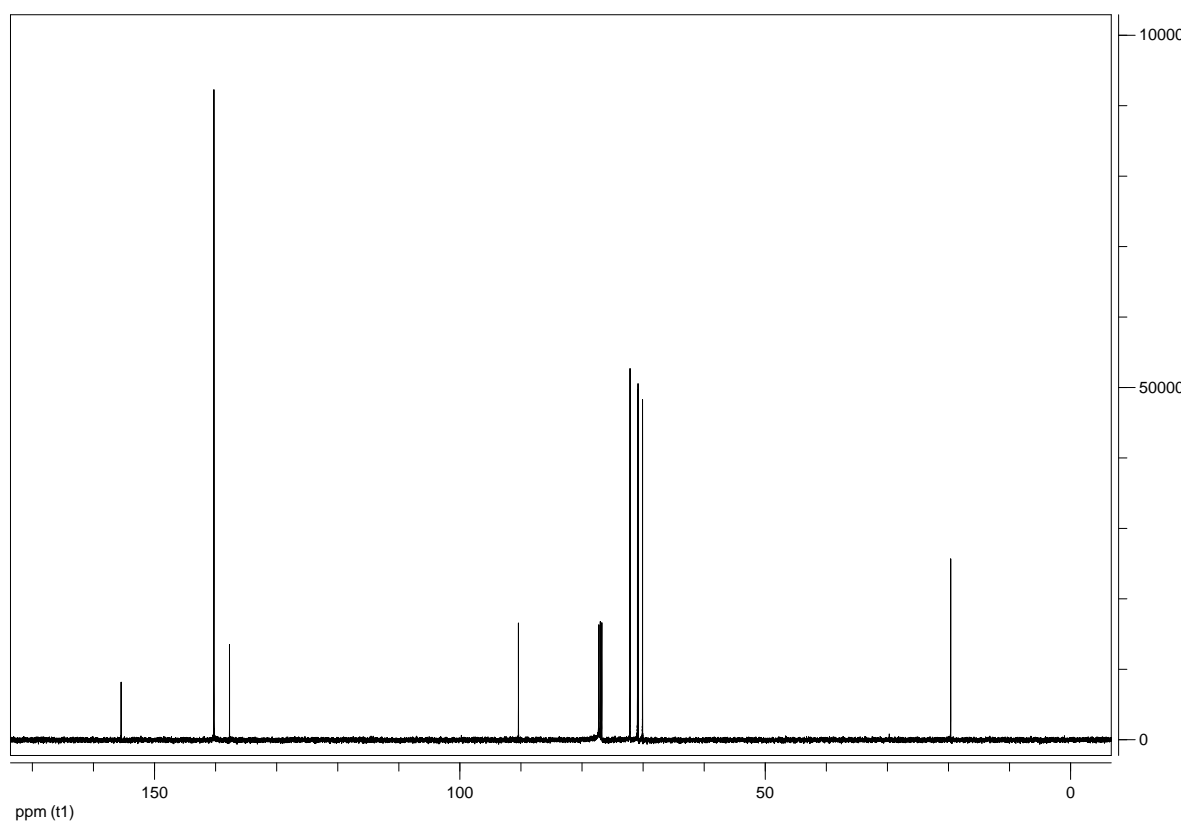
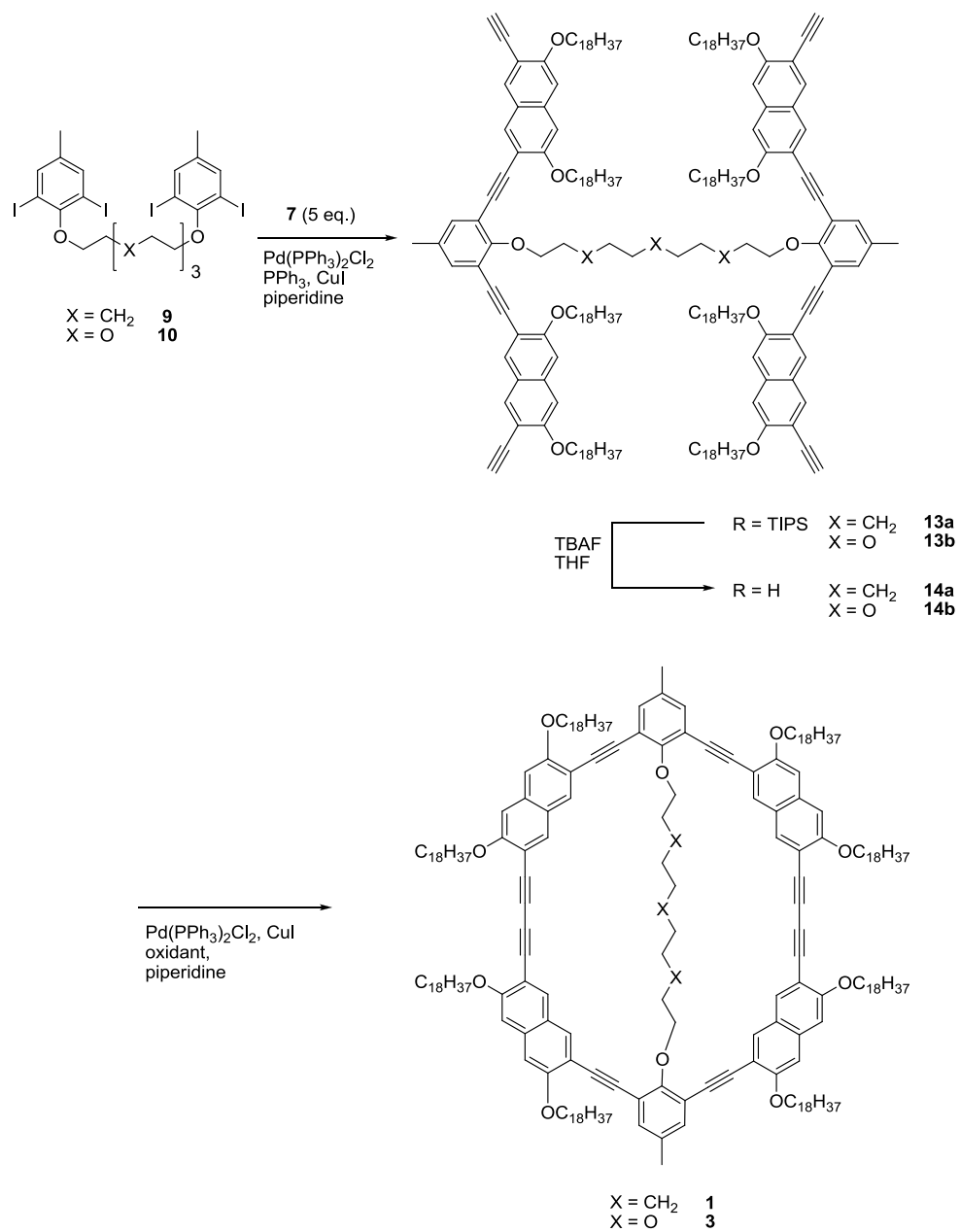


**Figure S27:**  $^{13}\text{C}$  NMR (125 MHz,  $\text{CDCl}_3$ ) of **10**.

### 8.3 Synthesis and characterization of macrocycles **1** and **3**



**Scheme S5:** Synthesis of **1** (oxidant: iodine) and **3** (oxidant: 1,4-benzoquinone).

**Synthesis of the TIPS-protected tetracetylene **13a**.** **9** (35 mg, 40  $\mu\text{mol}$ ), **7** (209 mg, 240  $\mu\text{mol}$ ), Pd(PPh<sub>3</sub>)Cl<sub>2</sub> (3.8 mg, 5.4  $\mu\text{mol}$ ), PPh<sub>3</sub> (3.5 mg, 13.3  $\mu\text{mol}$ ) and CuI (1.6 mg, 8.4  $\mu\text{mol}$ ) were dissolved in dry piperidine (1 mL) and heated to 70 °C. The mixture was stirred for 21 h and after cooling to room temperature diluted with CH<sub>2</sub>Cl<sub>2</sub> and water. The organic layer was extracted with water (3x), aqueous acetic acid (10 %, v/v), aqueous NaOH (10 %, w/w), and brine. After drying over MgSO<sub>4</sub> the solvent was evaporated. The product was purified by column chromatography (silica gel, petroleum ether : CH<sub>2</sub>Cl<sub>2</sub> = 3 : 1, *R<sub>f</sub>* = 0.25 (petroleum ether : CH<sub>2</sub>Cl<sub>2</sub> = 2 : 1)) yielding **13a** as a colorless solid (144 mg, 37.5  $\mu\text{mol}$ , 94 %). M.p. 73 °C. <sup>1</sup>H NMR (400 MHz, CDCl<sub>3</sub>):  $\delta$  [ppm] = 7.79 (d, *J* = 7.43 Hz, 8H), 7.28 (s, 4H), 6.90 (d, *J* = 3.01 Hz, 8H), 4.35 (t, *J* = 6.38 Hz, 4H), 4.04 (m, 16H), 2.29 (s, 6H), 1.83 (m, 18H), 1.59–1.20 (m, 252H), 1.19–1.07 (m, 84H), 0.91–0.81 (m, 24H). <sup>13</sup>C NMR (100 MHz, CDCl<sub>3</sub>): 158.983, 158.310, 157.782, 135.761, 134.194, 133.620, 132.919, 132.373, 122.920, 117.951, 112.825, 112.793, 105.383, 105.122, 103.331, 94.453, 90.126, 89.786, 74.669, 68.658, 68.611, 32.096, 30.779, 29.892, 29.838, 29.763, 29.725, 29.536, 29.371, 26.512, 26.347, 22.855, 20.564, 18.897, 14.276, 11.585. MALDI-MS (DCTB): *m/z* = 3838.2 (M)<sup>+</sup>, C<sub>261</sub>H<sub>428</sub>O<sub>10</sub>Si<sub>4</sub> requires 3835.21.

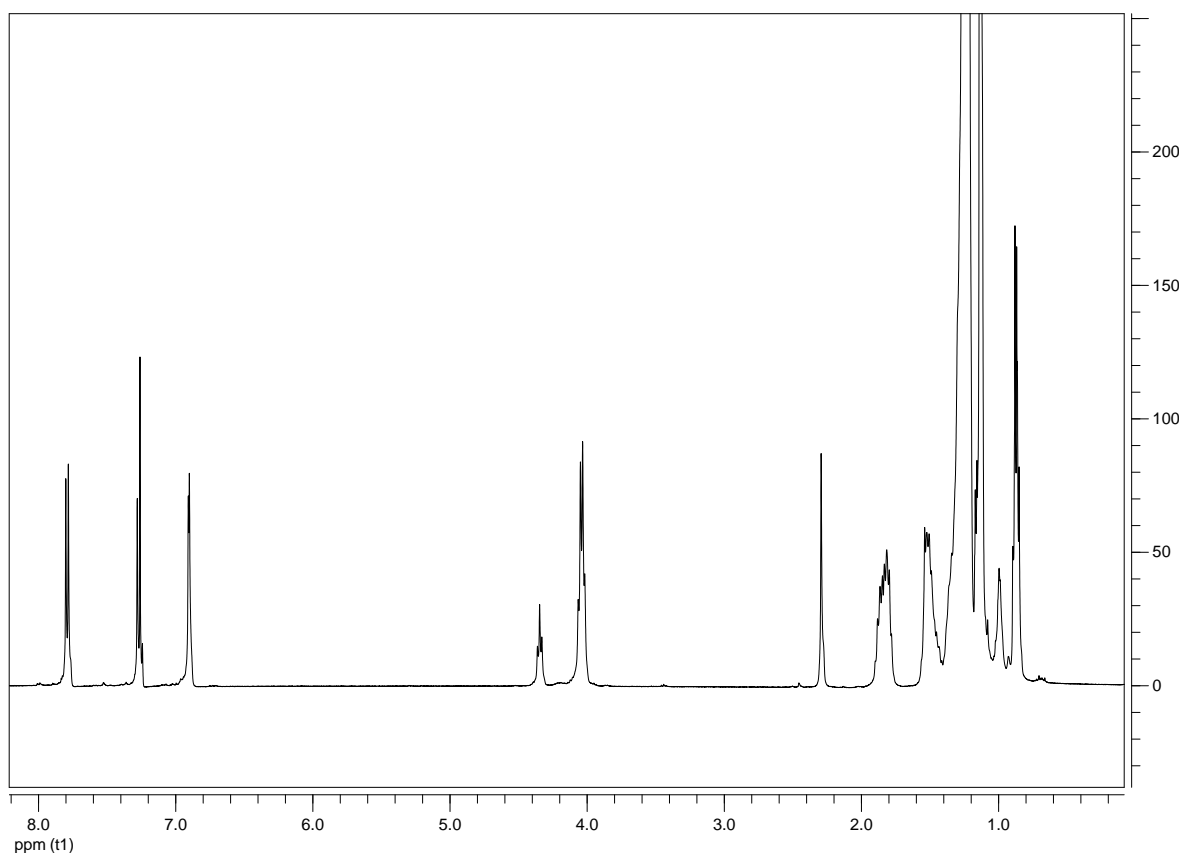


**Figure S28:** <sup>1</sup>H NMR (400 MHz, CDCl<sub>3</sub>) of **13a**.

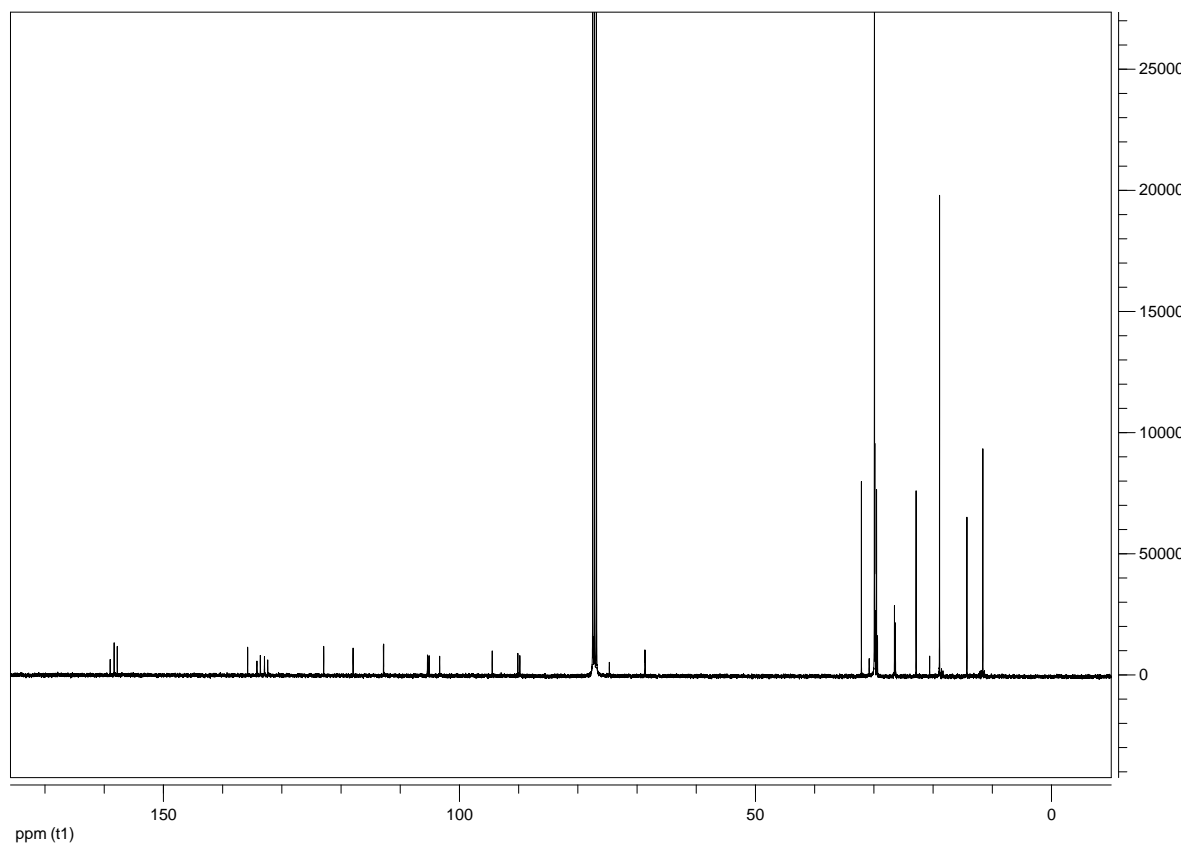


**Figure S29:**  $^1\text{H}$  NMR (100 MHz,  $\text{CDCl}_3$ ) of **13a**.

**Synthesis of the TIPS-protected tetraacetylene **13b**.** **10** (58 mg, 66.0  $\mu\text{mol}$ ), **7** (281 mg, 323  $\mu\text{mol}$ ), Pd(PPh<sub>3</sub>)Cl<sub>2</sub> (11.7 mg, 16.6  $\mu\text{mol}$ ), PPh<sub>3</sub> (6.3 mg, 24.0  $\mu\text{mol}$ ), and CuI (2.5 mg, 13.1  $\mu\text{mol}$ ) were dissolved in dry piperidine (2 mL). The mixture was stirred at 70 °C for 16 h and after cooling to room temperature diluted with CH<sub>2</sub>Cl<sub>2</sub> and water. The organic layer was extracted with water (3x), aqueous acetic acid (10 %, v/v), aqueous NaOH (10 %, w/w), and brine. After drying (MgSO<sub>4</sub>), the solvent was removed under reduced pressure. The crude product was purified by column chromatography (silica gel, CH<sub>2</sub>Cl<sub>2</sub> : MeOH = 50 : 1, R<sub>f</sub> = 0.28) yielding **13b** as a colorless oil (136 mg, 35.4  $\mu\text{mol}$ , 54 %). <sup>1</sup>H NMR (400 MHz, CDCl<sub>3</sub>):  $\delta$  [ppm] = 7.79 (s, 4H), 7.78 (s, 4H), 7.25 (s, 4H), 6.89 (s, 4H), 6.88 (s, 4H), 4.51 (t, *J* = 5.30 Hz, 4H), 4.03 (m, 16H), 3.88 (t, *J* = 5.32 Hz, 4H), 3.61–3.52 (m, 4H), 3.41–3.30 (m, 4H), 2.27 (s, 6H), 1.92–1.77 (m, 16H), 1.59–1.44 (m, 16H), 1.41–1.18 (m, 240H), 1.18–1.11 (m, 84H), 0.87 (m, 24H). <sup>13</sup>C NMR (100 MHz, CDCl<sub>3</sub>): 158.80, 158.28, 157.74, 135.76, 134.05, 133.66, 132.99, 132.59, 122.90, 117.80, 112.78, 112.68, 105.37, 105.11, 103.35, 94.43, 90.39, 89.58, 73.28, 70.77, 70.72, 70.63, 68.66, 68.59, 32.09, 29.90, 29.84, 29.78, 29.71, 29.57, 29.54, 29.33, 26.52, 26.32, 22.86, 20.55, 18.91, 14.28, 11.59. MALDI-MS (DCTB): *m/z* = 3844.4 (M<sup>+</sup>), 3867.6 (M+Na)<sup>+</sup>, C<sub>258</sub>H<sub>422</sub>O<sub>13</sub>Si<sub>4</sub> requires 3841.14.

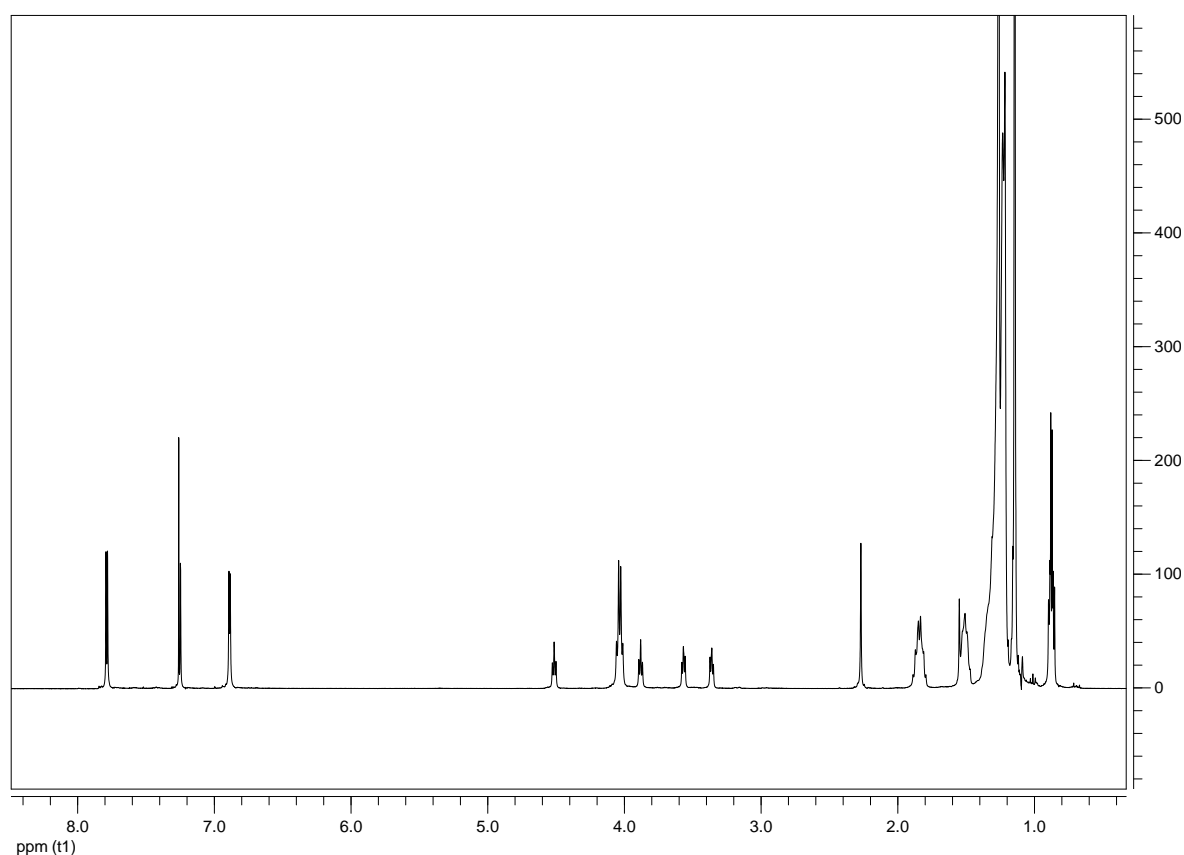


**Figure S30:** <sup>1</sup>H NMR (400 MHz, CDCl<sub>3</sub>) of **13b**.

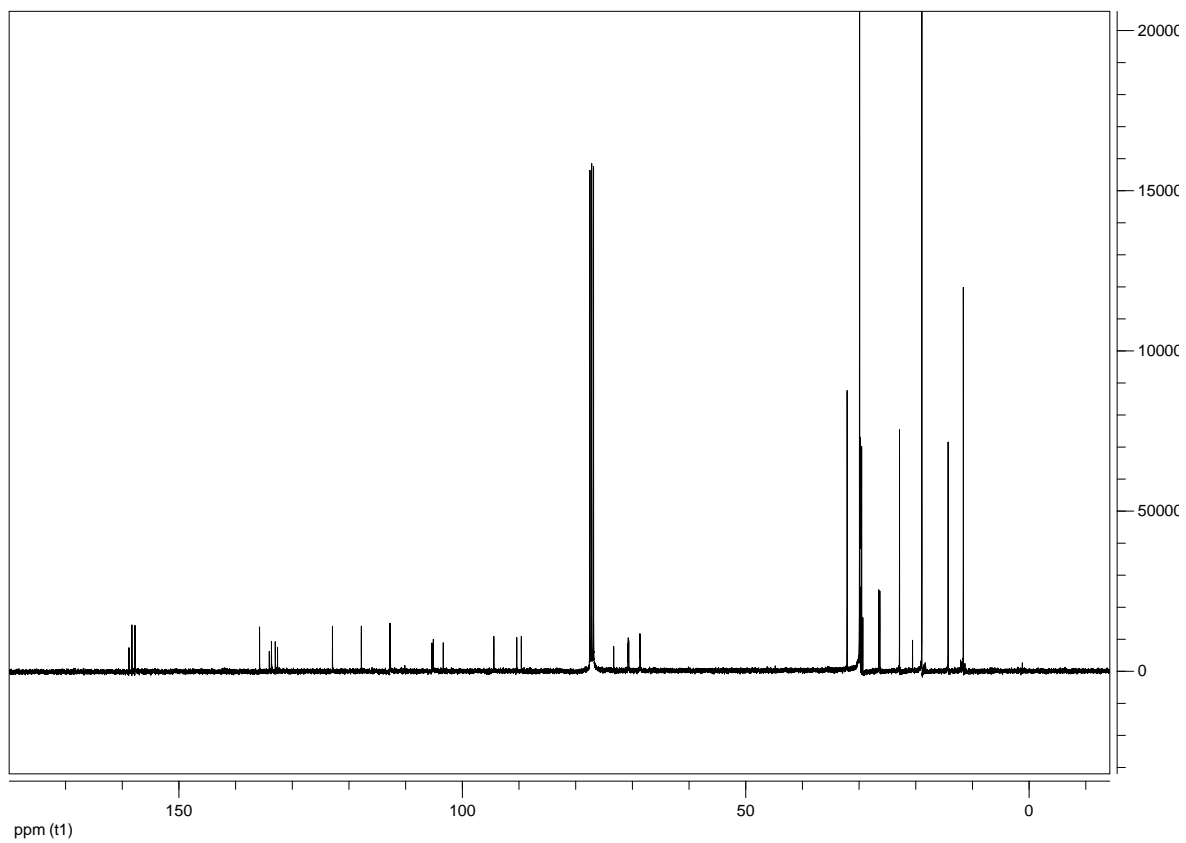


**Figure S31:**  $^{13}\text{C}$  NMR (100 MHz,  $\text{CDCl}_3$ ) of **13b**.

**Synthesis of the tetraacetylene **14a**.** To **13a** (144 mg, 37.5  $\mu\text{mol}$ ), dissolved in THF (4 mL), TBAF (1 M in THF, 0.3 mL) was added. The mixture was stirred for 2 h at room temperature. The reaction mixture was diluted with  $\text{CH}_2\text{Cl}_2$  and extracted with water (3x) and brine. The organic phase was dried over  $\text{MgSO}_4$ , and the solvent was evaporated. The residue was dissolved in  $\text{CH}_2\text{Cl}_2$  and precipitated with MeOH to yield **14a** as a colorless solid (107 mg, 33.3  $\mu\text{mol}$ , 89 %). M.p. 68°C.  $^1\text{H}$  NMR (400 MHz,  $\text{CDCl}_3$ ):  $\delta$  [ppm] = 7.82 (s, 4H), 7.80 (s, 4H), 7.30 (s, 4H), 6.94 (s, 4H), 6.93 (s, 4H), 4.36 (t,  $J$  = 6.27 Hz, 4H), 4.08 (m, 16H), 3.25 (s, 4H, acetylene-H), 2.30 (s, 6H), 1.97–1.79 (m, 20H), 1.61–1.44 (m, 20H), 1.44–1.00 (m, 250H), 0.87 (m, 24H).  $^{13}\text{C}$  NMR (100 MHz,  $\text{CDCl}_3$ ): 158.92, 157.84, 157.78, 135.77, 134.03, 132.87, 132.35, 122.71, 117.78, 112.83, 111.21, 105.28, 105.18, 89.85, 89.73, 80.77, 80.04, 74.61, 68.65, 68.55, 31.93, 30.74, 30.08, 30.02, 29.73, 29.67, 29.65, 29.61, 29.57, 29.41, 29.38, 29.19, 28.99, 26.58, 26.17, 26.00, 22.70, 20.42, 14.12. MALDI-MS (DCTB):  $m/z$  = 3212.6 ( $\text{M}^+$ ), 3462.7 ( $\text{M}+\text{DCTB}$ ) $^+$ ,  $\text{C}_{225}\text{H}_{348}\text{O}_{10}$  requires 3210.67. GPC (PS calibration): single peak at  $M_{\text{peak}} = 4.80 \times 10^3 \text{ g mol}^{-1}$ .

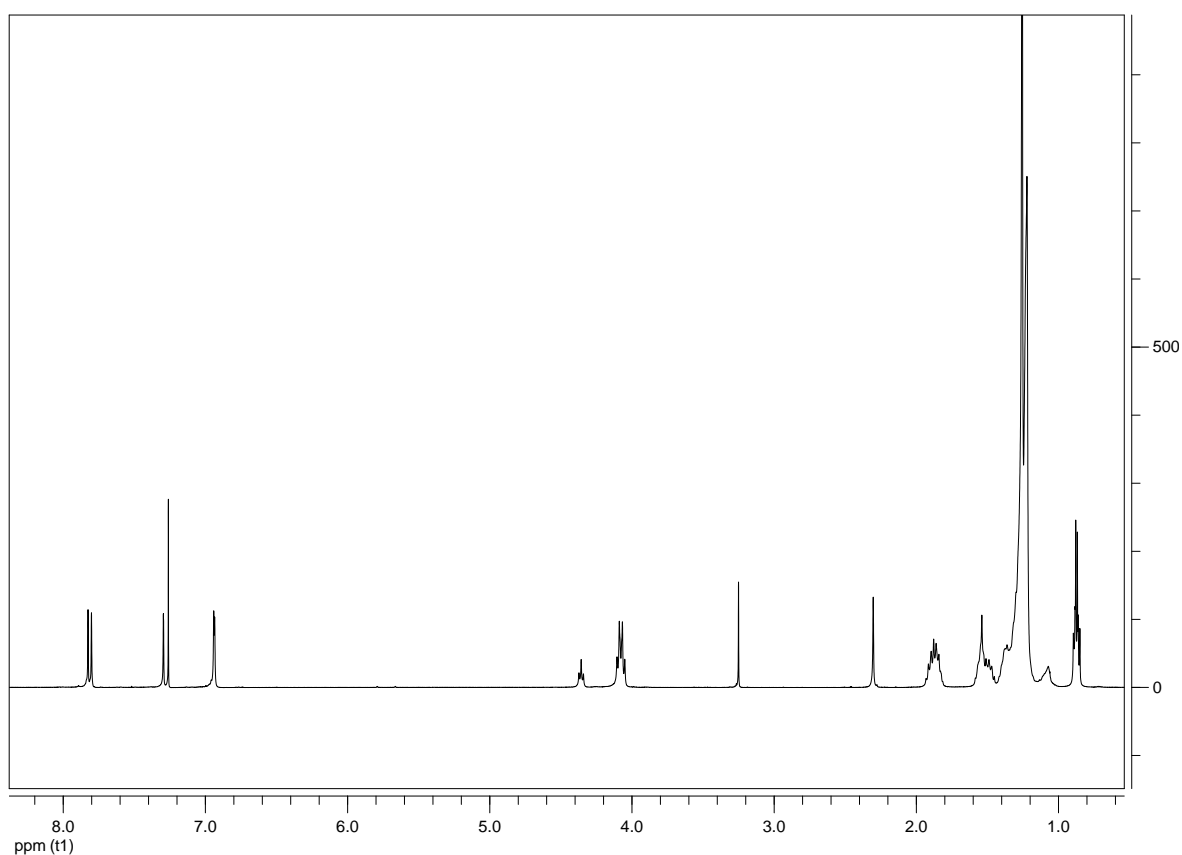


**Figure S32:**  $^1\text{H}$  NMR (400 MHz,  $\text{CDCl}_3$ ) of **14a**.

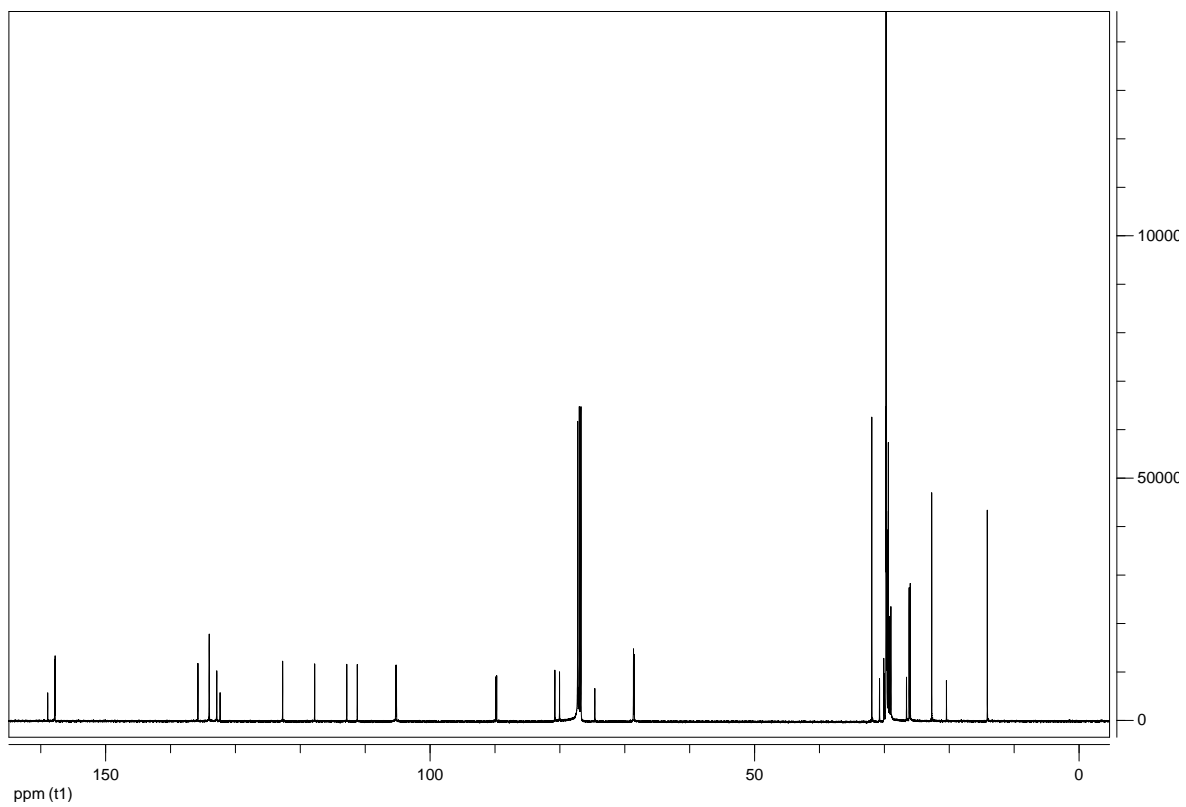


**Figure S33:**  $^{13}\text{C}$  NMR (100 MHz,  $\text{CDCl}_3$ ) of **14a**.

**Synthesis of the tetraacetylene **14b**.** **13b** (136 mg, 35.4  $\mu\text{mol}$ ) was dissolved in THF (2 mL) and TBAF (1 M in THF, 0.35 mL) was added. The mixture was stirred for 24 h at room temperature. Subsequently the reaction mixture was diluted with  $\text{CH}_2\text{Cl}_2$  and extracted with water (3x) and brine. The organic phase was dried over  $\text{MgSO}_4$ , and the solvent was evaporated. The crude product was purified by column chromatography (silica gel,  $\text{CH}_2\text{Cl}_2$ ,  $R_f = 0.1$  (DCM : MeOH = 100 : 1)) to yield **14b** as a slightly yellow solid (107 mg, 33.3  $\mu\text{mol}$ , 94 %). M.p. 79 °C.  $^1\text{H}$  NMR (400 MHz,  $\text{CD}_2\text{Cl}_2$ ):  $\delta$  [ppm] = 7.83 (s, 4H), 7.82 (s, 4H), 7.28 (s, 4H), 6.97 (s, 8H), 4.51 (t,  $J = 5.03$  Hz, 4H), 4.09 (m, 16H), 3.89 (t,  $J = 5.05$  Hz, 4H), 3.60 (t,  $J = 4.97$  Hz, 4H), 3.44 (t,  $J = 4.97$  Hz, 4H), 3.27 (s, 4H), 2.30 (s, 6H), 1.98–1.77 (m, 16H), 1.61–1.45 (m, 16H), 1.45–0.99 (m, 240H), 0.99–0.58 (m, 24H).  $^{13}\text{C}$  NMR (125 MHz,  $\text{CD}_2\text{Cl}_2$ ): 158.70, 157.96, 157.84, 135.10, 134.07, 134.01, 133.00, 132.92, 122.69, 117.62, 112.63, 111.19, 105.36, 105.25, 90.23, 89.49, 80.68, 80.14, 73.37, 70.83, 70.66, 70.52, 68.75, 68.71, 32.02, 29.81, 29.76, 29.74, 29.71, 29.65, 29.50, 29.47, 29.25, 29.12, 26.25, 26.09, 22.78, 20.26, 13.97. MALDI-MS (DCTB):  $m/z = 3216.6$  ( $\text{M}^+$ ), 3239.6 ( $\text{M}+\text{Na}^+$ ), 3255.7 ( $\text{M}+\text{K}^+$ ),  $\text{C}_{222}\text{H}_{342}\text{O}_{13}$  requires 3216.61. GPC (PS calibration): single peak at  $M_{\text{peak}} = 4.72 \times 10^3$  g  $\text{mol}^{-1}$ .

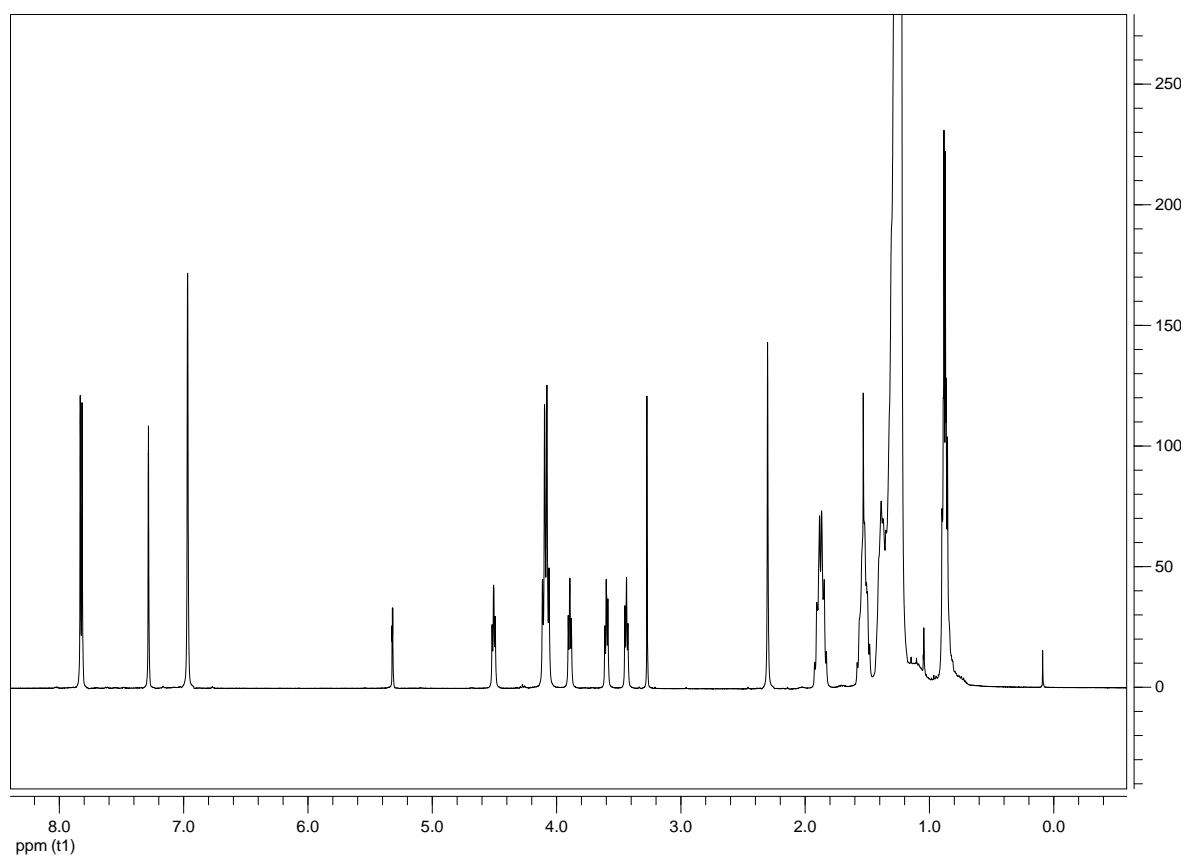


**Figure S34:**  $^1\text{H}$  NMR (400 MHz,  $\text{CDCl}_3$ ) of **14b**.

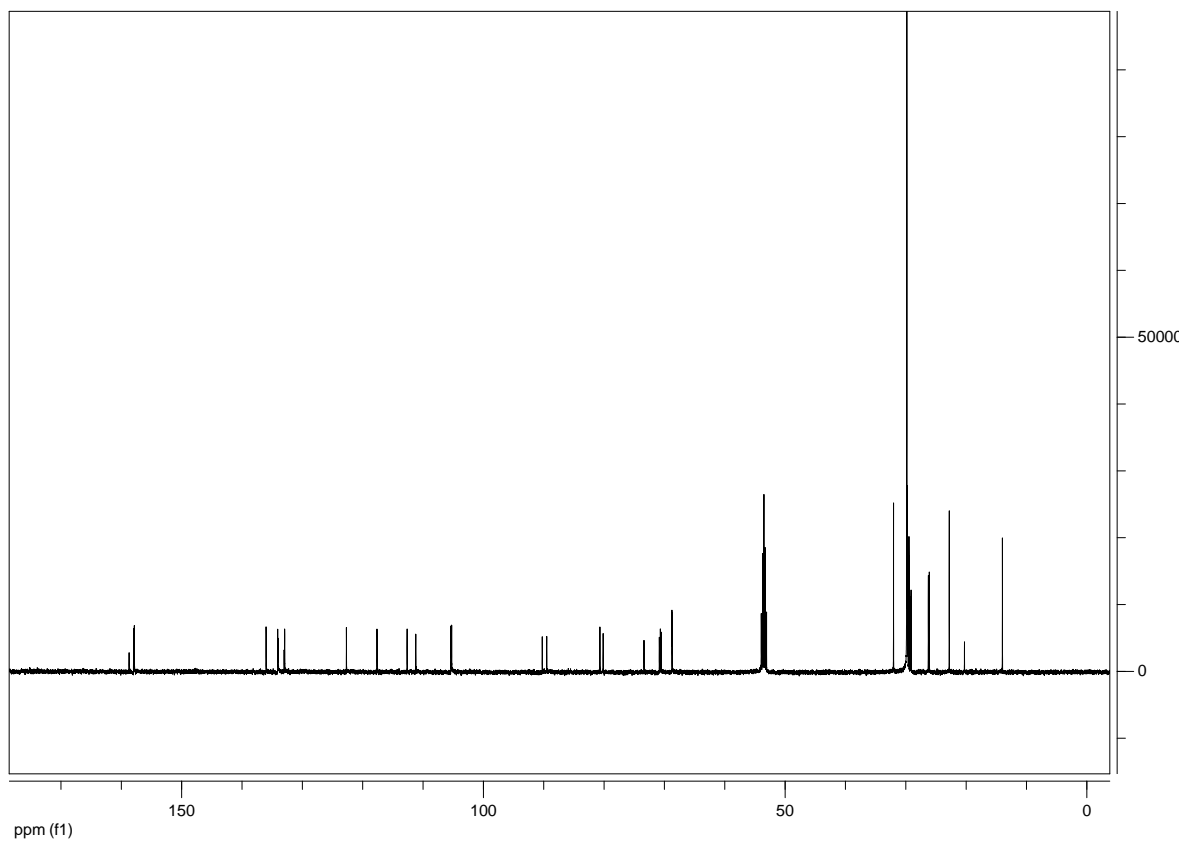


**Figure S35:**  $^{13}\text{C}$  NMR (100 MHz,  $\text{CDCl}_3$ ) of **14b**.

**Synthesis of macrocycle 1.** The coupling was performed according to procedures reported previously.<sup>[6a, 6b, 9]</sup> A 50 ml Hamilton syringe was charged with a solution of tetraacetylene **14a** (30.5 mg, 9.49  $\mu\text{mol}$ ) in THF (15 mL). Pd(PPh<sub>3</sub>)<sub>2</sub>Cl<sub>2</sub> (3.6 mg, 5.13  $\mu\text{mol}$ ) and CuI (34.65  $\mu\text{mol}$ ) together with iodine (7.5 mg, 29.54  $\mu\text{mol}$ ) were dissolved in THF (15 mL) and piperidine (15 mL) and heated to 50 °C. While stirring vigorously, the acetylene-solution was added dropwise to the catalyst/oxidant-solution over a period of 48 h. The mixture was stirred for additional 44 h at 50 °C. The reaction mixture was diluted with CHCl<sub>3</sub> and water. The organic layer was extracted with water (3x), acetic acid (10 % v/v, 3x), water, NaOH (10 % w/w), and brine, and subsequently dried over MgSO<sub>4</sub>. The solvent was removed under reduced pressure. The residue was dissolved in CH<sub>2</sub>Cl<sub>2</sub> and the product was precipitated with MeOH. The suspension was filtered through a PTFE-membrane to yield **1** as a slightly yellow solid (16.5 mg, 5.14  $\mu\text{mol}$ , 54 %). M.p. 168 °C. <sup>1</sup>H NMR (400 MHz, CDCl<sub>3</sub>):  $\delta$  [ppm] = 7.99 (s, 4H), 7.78 (s, 4H), 7.29 (s, 4H), 6.96 (s, 8H), 4.38 (t,  $J = 7.07$  Hz, 4H), 4.19–4.09 (m, 16H), 2.31 (s, 6H), 2.20–2.09 (m, 4H), 2.01–1.89 (m, 16H), 1.76–1.16 (m, 254H), 0.94–0.78 (m, 24H). MALDI-MS (DCTB):  $m/z = 3206.6$  (M<sup>+</sup>),  $6416 \pm 10$  ([2M]<sup>+</sup>). C<sub>225</sub>H<sub>344</sub>O<sub>10</sub> requires 3206.64. GPC (PS calibration): single peak at  $M_{\text{peak}} = 4.44 \times 10^3$  g mol<sup>-1</sup>.

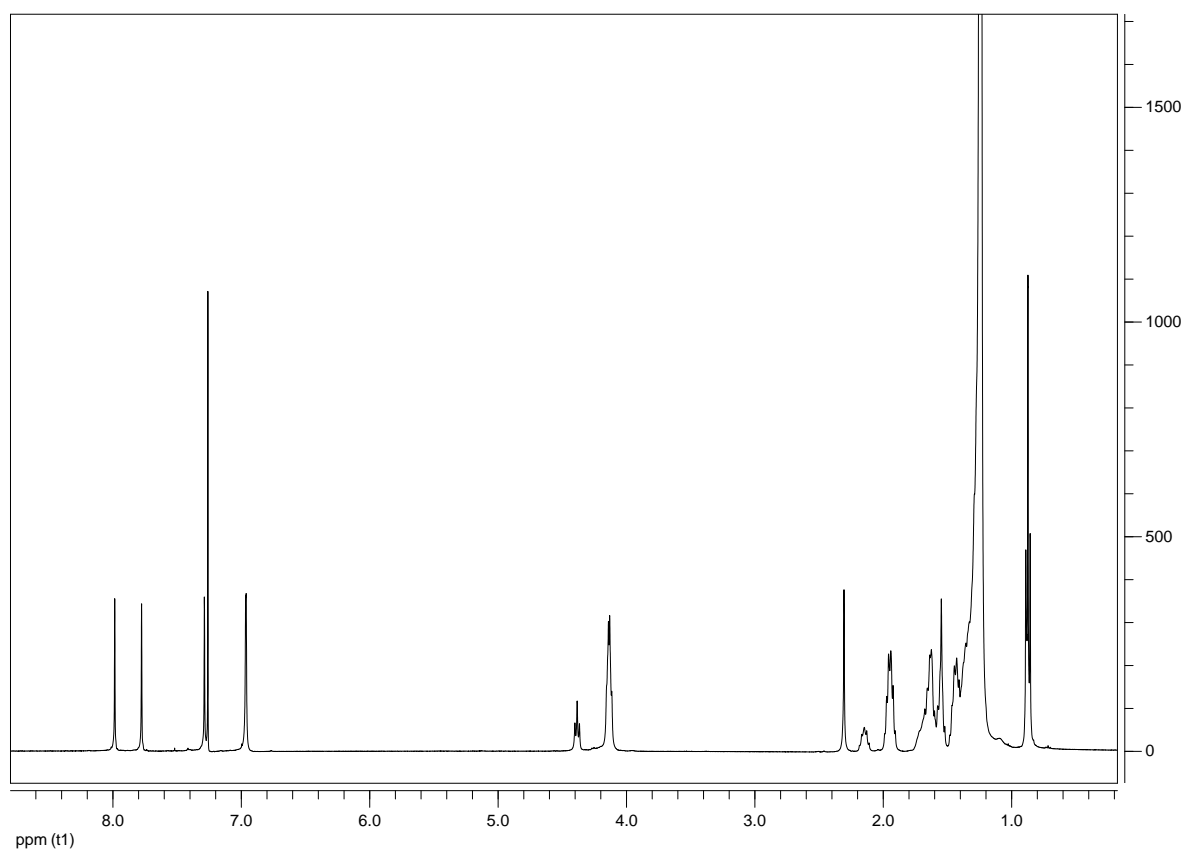


**Figure S36:** <sup>1</sup>H NMR (400 MHz, CDCl<sub>3</sub>) of **2**.

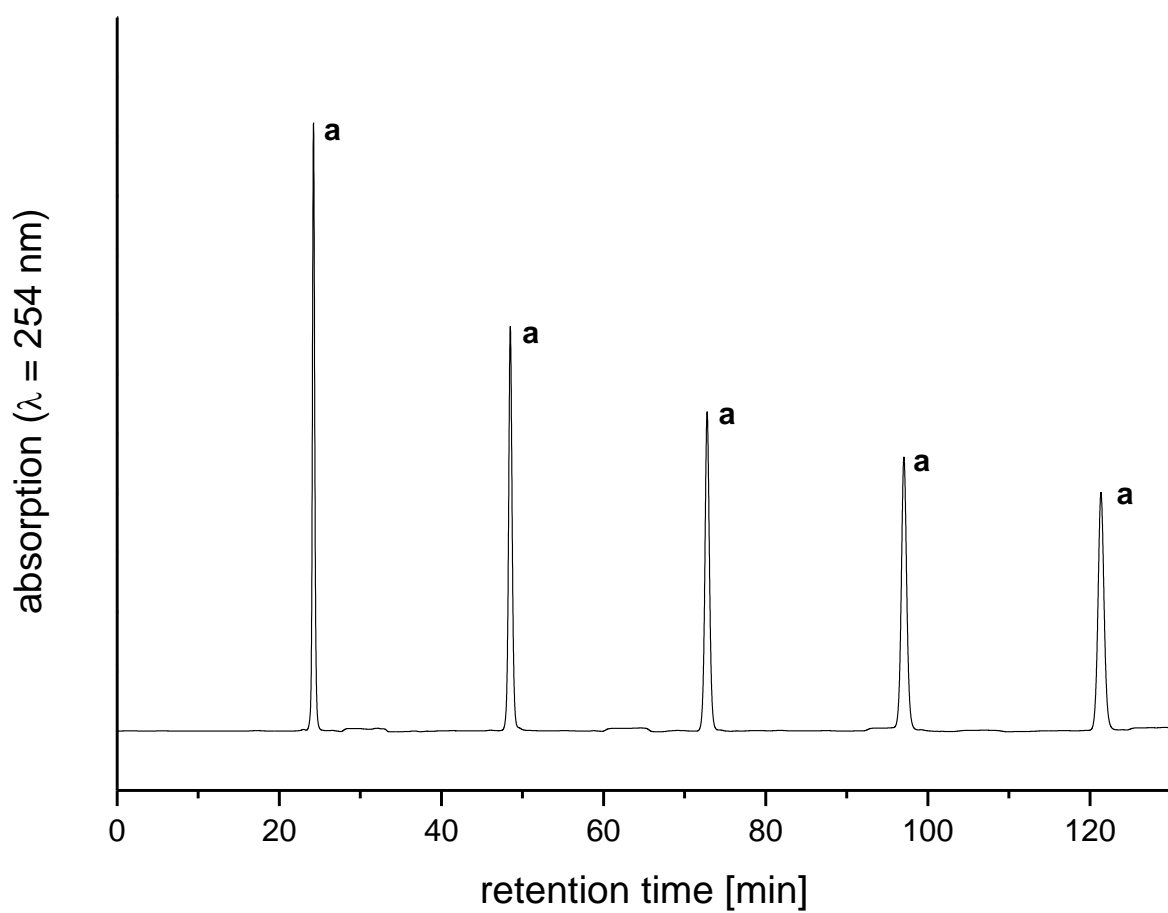


**Figure S37:** Recycling GPC elugram of **1**. In the cyclization step no detectable oligomers are formed. Thus, only one signal (**a**), attributed to the macrocycle **1**, is observed in the elugram.

**Synthesis of macrocycle 3.** The procedure follows the synthesis of **1**. However, the Glaser coupling protocol was varied slightly.<sup>[10]</sup> A 50 ml Hamilton syringe was charged with a solution of tetraacetylene **14b** (44.2 mg, 13.73  $\mu\text{mol}$ ) in THF (10 mL). Pd(PPh<sub>3</sub>)<sub>2</sub>Cl<sub>2</sub> (5.5 mg, 7.84  $\mu\text{mol}$ ), CuI (5.1 mg, 26.78  $\mu\text{mol}$ ) and 1,4-benzoquinone (8.0 mg, 74.01  $\mu\text{mol}$ ) were dissolved in THF (15 mL) and piperidine (10 mL), and heated to 50 °C. While stirring vigorously, the acetylene-solution was added dropwise to the catalyst/oxidant-solution over a period of 72 h. The mixture was stirred for additional 24 h at 50 °C. The reaction mixture was diluted with CH<sub>2</sub>Cl<sub>2</sub> and water. The organic layer was extracted with water (3x), acetic acid (10 % v/v, 3x), water, 2 M NaOH and brine, and was dried over MgSO<sub>4</sub>. The solvent was evaporated under reduced pressure. Inorganic compounds were removed by column chromatography (CH<sub>2</sub>Cl<sub>2</sub>,  $R_f$  = 0.99). The resulting crude product was purified by preparative recycling GPC to yield **3** as a slightly yellow solid (10.4 mg, 3.23  $\mu\text{mol}$ , 24 %). M.p. 181 °C. <sup>1</sup>H NMR (400 MHz, CD<sub>2</sub>Cl<sub>2</sub>):  $\delta$  [ppm] = 8.05 (s, 4H), 7.81 (s, 4H), 7.31 (s, 4H), 6.97 (s, 4H), 6.96 (s, 4H), 4.63–4.55 (m, 4H), 4.22–4.09 (m, 22H), 3.99–3.92 (m, 8H), 2.30 (s, 6H), 2.00–1.89 (m, 16H), 1.69–1.49 (m, 16H), 1.49–1.16 (m, 240H), 0.92–0.82 (m, 24H). <sup>13</sup>C NMR (125 MHz, CDCl<sub>3</sub>):  $\delta$  [ppm] = 158.25, 157.76, 157.71, 136.69, 136.09, 134.84, 132.95, 132.50, 123.14, 117.60, 112.90, 111.50, 105.53, 105.32, 90.18, 89.91, 80.39, 78.20, 77.36, 72.40, 71.13, 70.63, 70.21, 69.00, 68.67, 32.10, 29.92, 29.89, 29.84, 29.81, 29.77, 29.58, 29.54, 29.45, 29.10, 26.46, 26.19, 22.86, 20.53, 14.29. MALDI-MS (DCTB):  $m/z$  = 3022.4 ([M–4EG]<sup>+</sup>), 3212.6 (M<sup>+</sup>), 3735.7 ([M+2 DCTB+Na]<sup>+</sup>) (C<sub>222</sub>H<sub>338</sub>O<sub>13</sub> requires 3212.58). GPC (PS calibration): single peak at  $M_{\text{peak}} = 4.89 \times 10^3 \text{ g mol}^{-1}$ .

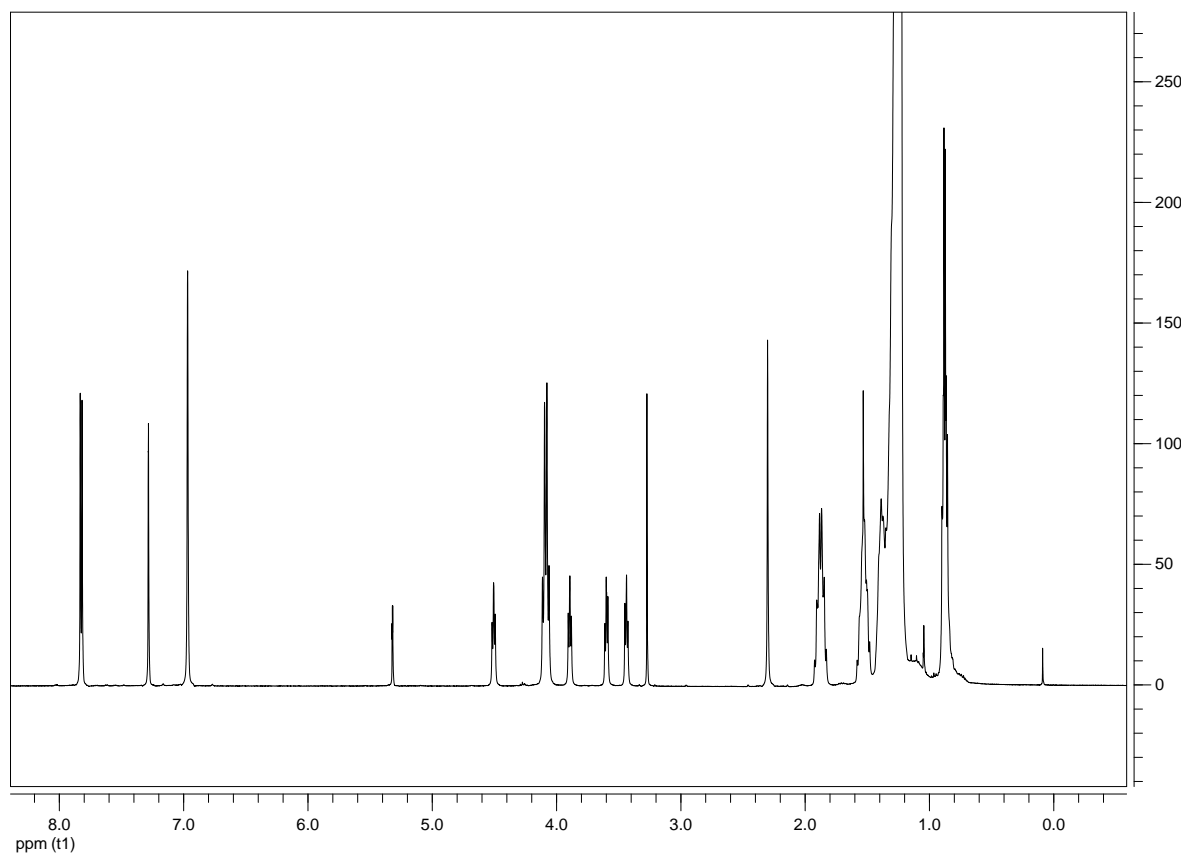


**Figure S38:**  $^1\text{H}$  NMR (400 MHz,  $\text{CD}_2\text{Cl}_2$ ) of **3**.

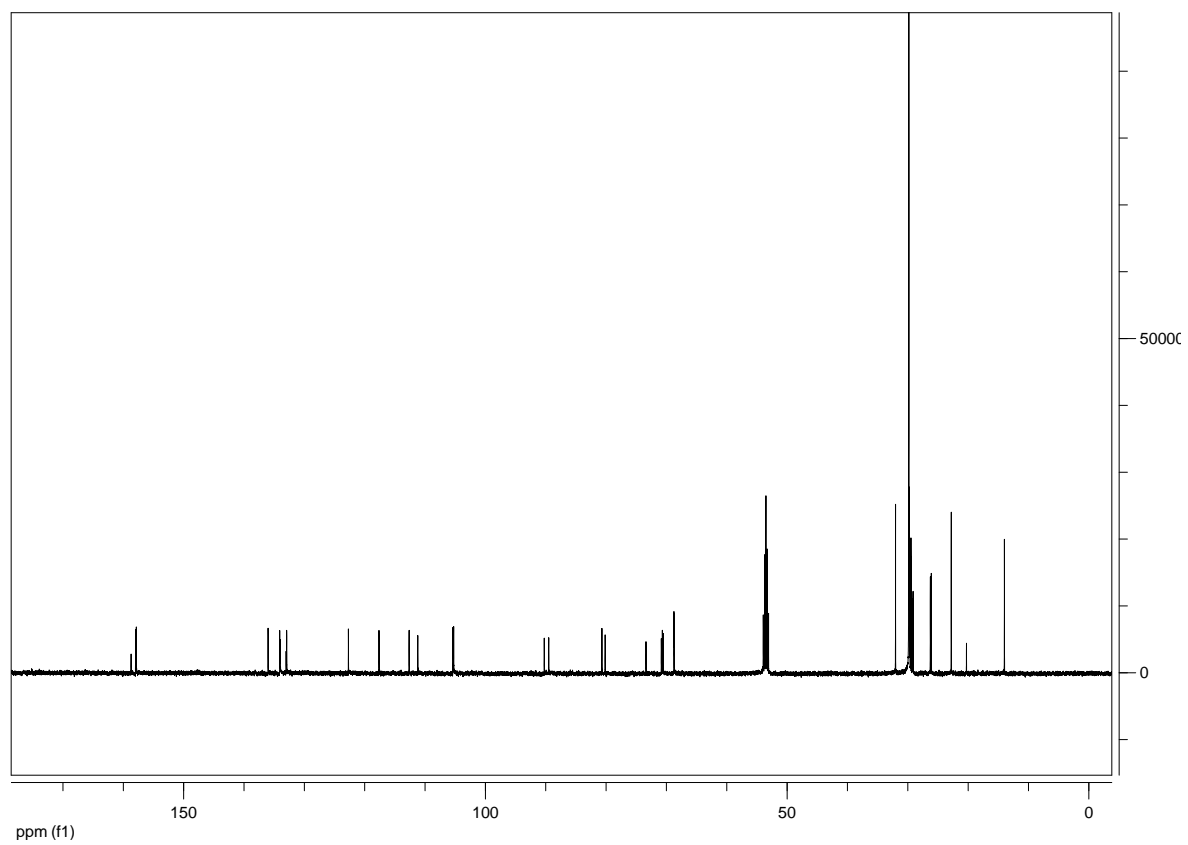


**Figure S39:**  $^{13}\text{C}$  NMR (125 MHz,  $\text{CDCl}_3$ ) of **3**.

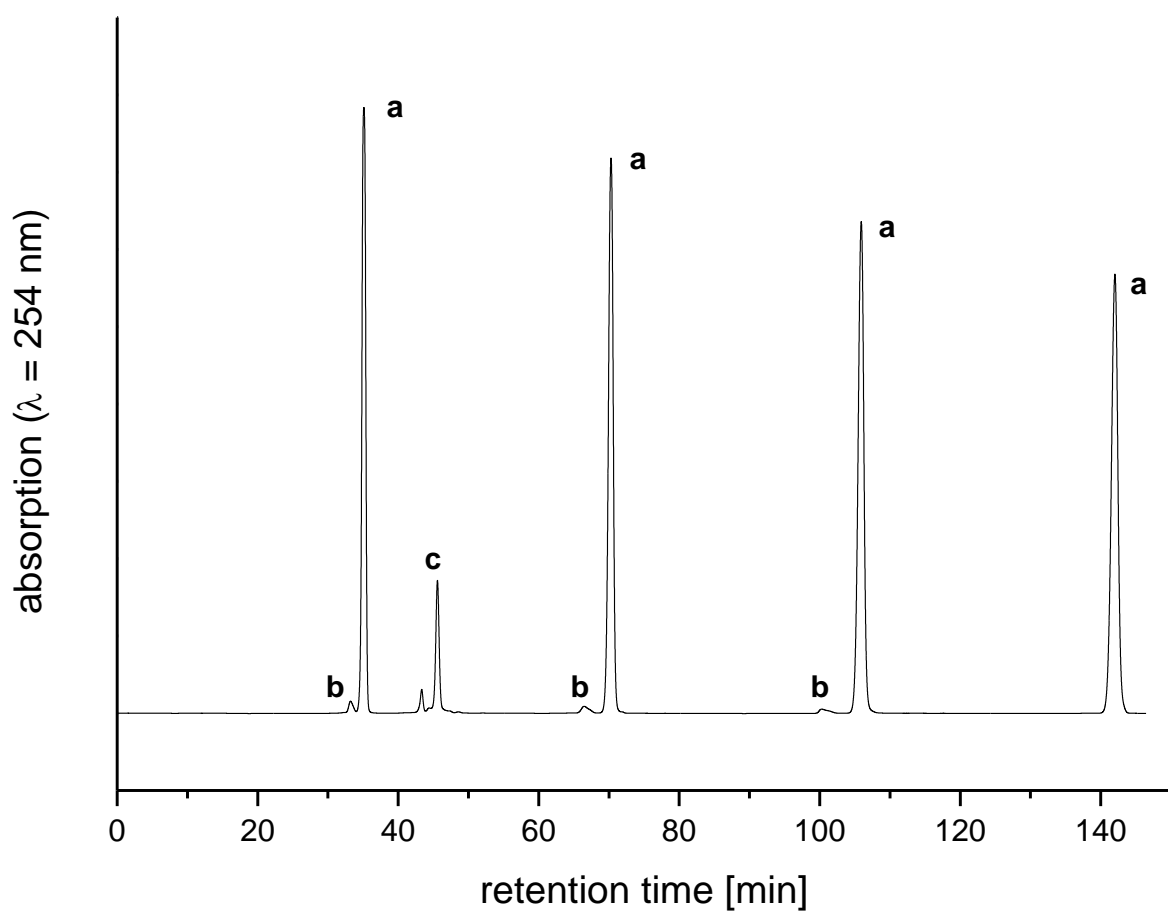
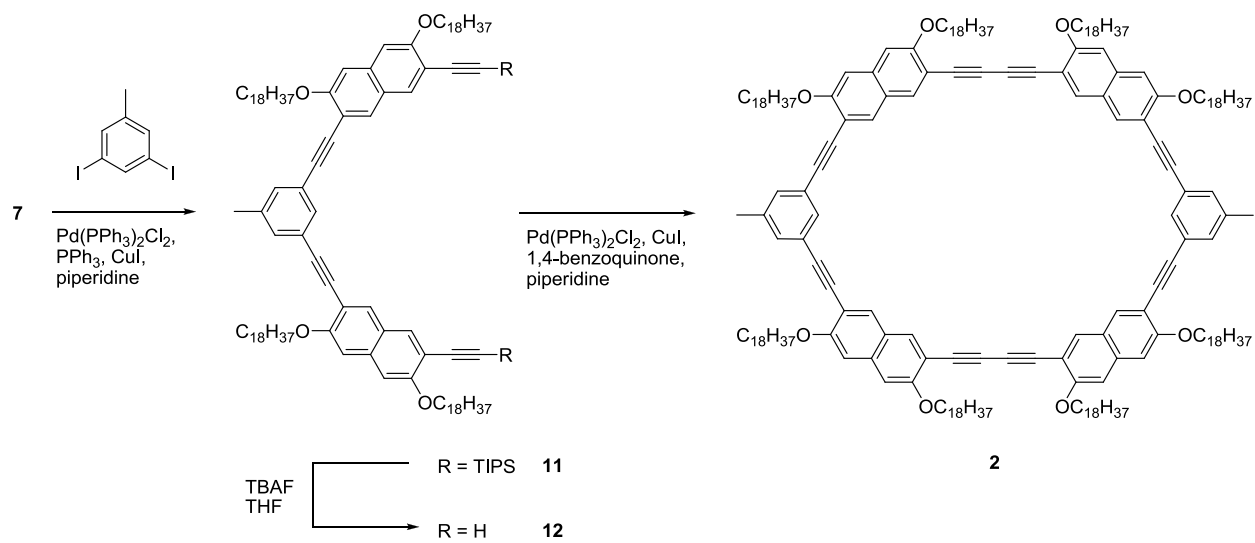


**Figure S40:** Recycling GPC elugram of **3**. Beside signal **a** (attributed to the macrocycle), only few additional signals (**b**, attributed to oligomeric byproducts, and **c**, attributed to low molecular mass impurities) are detected. After separating the impurities, the pure macrocycle **3** is isolated.

## 8.4 Synthesis and characterization of macrocycle 2



**Scheme S6:** Reaction pathway towards macrocycle 2.

**Synthesis of the TIPS-protected half-ring 11.** Pd(PPh<sub>3</sub>)Cl<sub>2</sub> (2.7 mg, 3.8 μmol), PPh<sub>3</sub> (1.8 mg, 6.9 μmol), and CuI (1.3 mg, 6.8 μmol) were added to a solution of **7** (171 mg, 197 μmol) and 3,5-diiodotoluene (28 mg, 81 μmol) in dry piperidine (2 mL). The mixture was stirred at 70 °C for 2 h. After cooling to room temperature, water and CH<sub>2</sub>Cl<sub>2</sub> were added. The organic layer was separated and extracted with water (3x), aqueous acetic acid (10 %, v/v), aqueous NaOH (10 %, w/w), and brine and dried over MgSO<sub>4</sub>. The solvent was removed under reduced pressure, and the residue was purified by column chromatography (silica gel, petroleum ether : CH<sub>2</sub>Cl<sub>2</sub> = 7 : 1, R<sub>f</sub> = 0.28) yielding **11** as a yellowish solid (144 mg, 78.8 μmol, 97 %). <sup>1</sup>H NMR (400 MHz, CDCl<sub>3</sub>): δ [ppm] = 7.84 (s, 2H), 7.83 (s, 2H), 7.57 (s, 1H), 7.34 (d, *J* = 0.54 Hz, 2H), 6.96 (s, 2H), 6.93 (s, 2H), 4.13 (t, *J* = 6.35 Hz, 4H), 4.07 (t, *J* = 6.20 Hz, 4H), 2.37 (s, 3H), 2.00–1.81 (m, 8H), 1.67–1.49 (m, 8H), 1.48–1.19 (m, 112H), 1.19–1.40 (m, 42H, TIPS), 0.88 (m, 12H). <sup>13</sup>C NMR (125 MHz, CDCl<sub>3</sub>): 158.33, 157.82, 138.13, 135.82, 133.71, 132.98, 132.07, 131.76, 124.01, 122.90, 112.81, 112.41, 105.38, 105.11, 103.30, 94.53, 92.77, 86.35, 68.68, 68.60, 32.10, 29.88, 29.84, 29.71, 29.70, 29.54, 29.51, 29.38, 26.48, 26.40, 22.86, 21.25, 18.91, 14.29, 11.59. MALDI-MS (DCTB): *m/z* = 1825.5 (M<sup>+</sup>), C<sub>125</sub>H<sub>204</sub>O<sub>4</sub>Si<sub>2</sub> requires 1825.53).

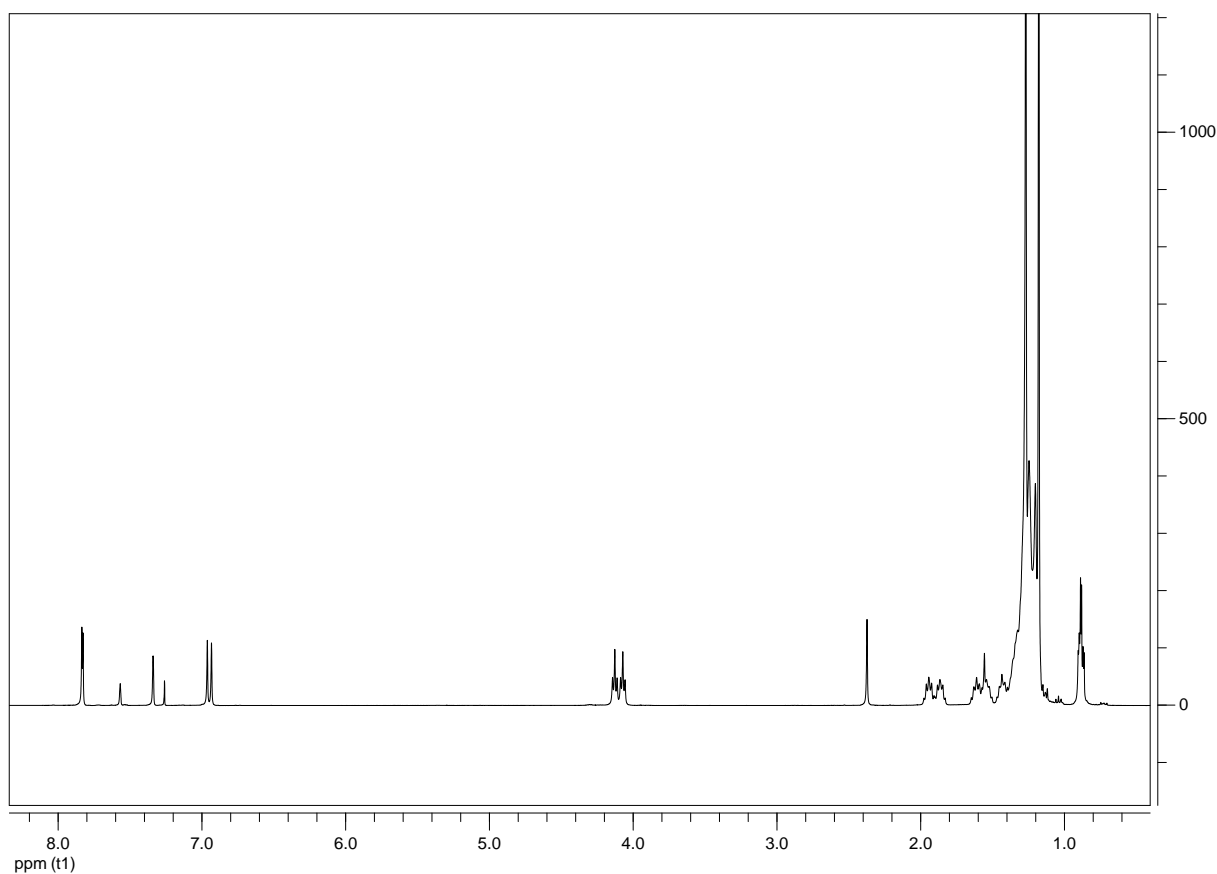


**Figure S41:** <sup>1</sup>H NMR (400 MHz, CDCl<sub>3</sub>) of **11**.

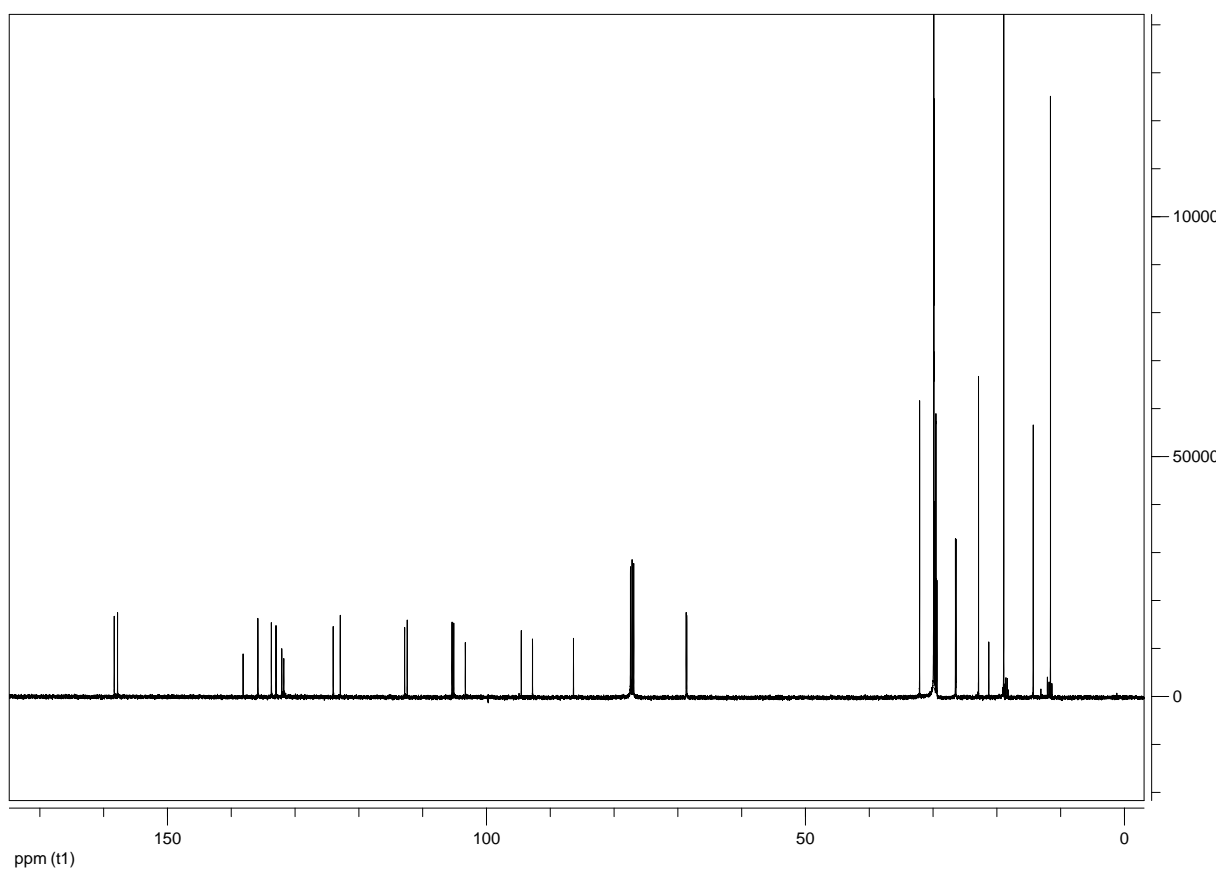


**Figure S42:**  $^{13}\text{C}$  NMR (100 MHz,  $\text{CDCl}_3$ ) of **11**.

**Synthesis of the bisacetylene **12**.** **11** (144 mg, 78.8  $\mu\text{mol}$ ) was dissolved in THF (1 mL), and TBAF (1 M in THF, 0.4 mL) was added. After stirring for 18 h, the reaction mixture was diluted with  $\text{CH}_2\text{Cl}_2$  and extracted with water (3x) and brine. The organic layer was dried over  $\text{MgSO}_4$ , and the solvent was removed under reduced pressure. The residue was dissolved in  $\text{CH}_2\text{Cl}_2$  and reprecipitated with MeOH to yield **12** as a colorless solid (110 mg, 72.2  $\mu\text{mol}$ , 92 %). M.p. 78°C.  $^1\text{H}$  NMR (300 MHz,  $\text{CDCl}_3$ ):  $\delta$  [ppm] = 7.86 (s, 2H), 7.84 (s, 2H), 7.57 (s, 1H), 7.38–7.31 (m, 2H), 6.97 (s, 4H), 4.18–4.06 (m, 8H), 3.28 (s, 2H), 2.37 (s, 3H), 2.03–1.81 (m, 8H), 1.70–1.47 (m, 8H), 1.48–1.11 (m, 112H), 0.94–0.82 (m, 12H).  $^{13}\text{C}$  NMR (75 MHz,  $\text{CDCl}_3$ ): 158.07, 158.03, 138.17, 136.02, 134.25, 133.03, 132.12, 131.81, 123.97, 122.88, 112.73, 111.39, 110.14, 105.51, 105.40, 92.92, 86.24, 80.79, 80.26, 68.86, 68.76, 32.09, 30.05, 30.02, 30.00, 29.87, 29.77, 29.75, 29.69, 29.54, 29.36, 29.14, 26.39, 26.16, 22.85, 21.25, 14.28. MALDI-MS (DCTB):  $m/z$  = 1513.2 ( $\text{M}^+$ ),  $\text{C}_{107}\text{H}_{164}\text{O}_4$  requires 1513.26).

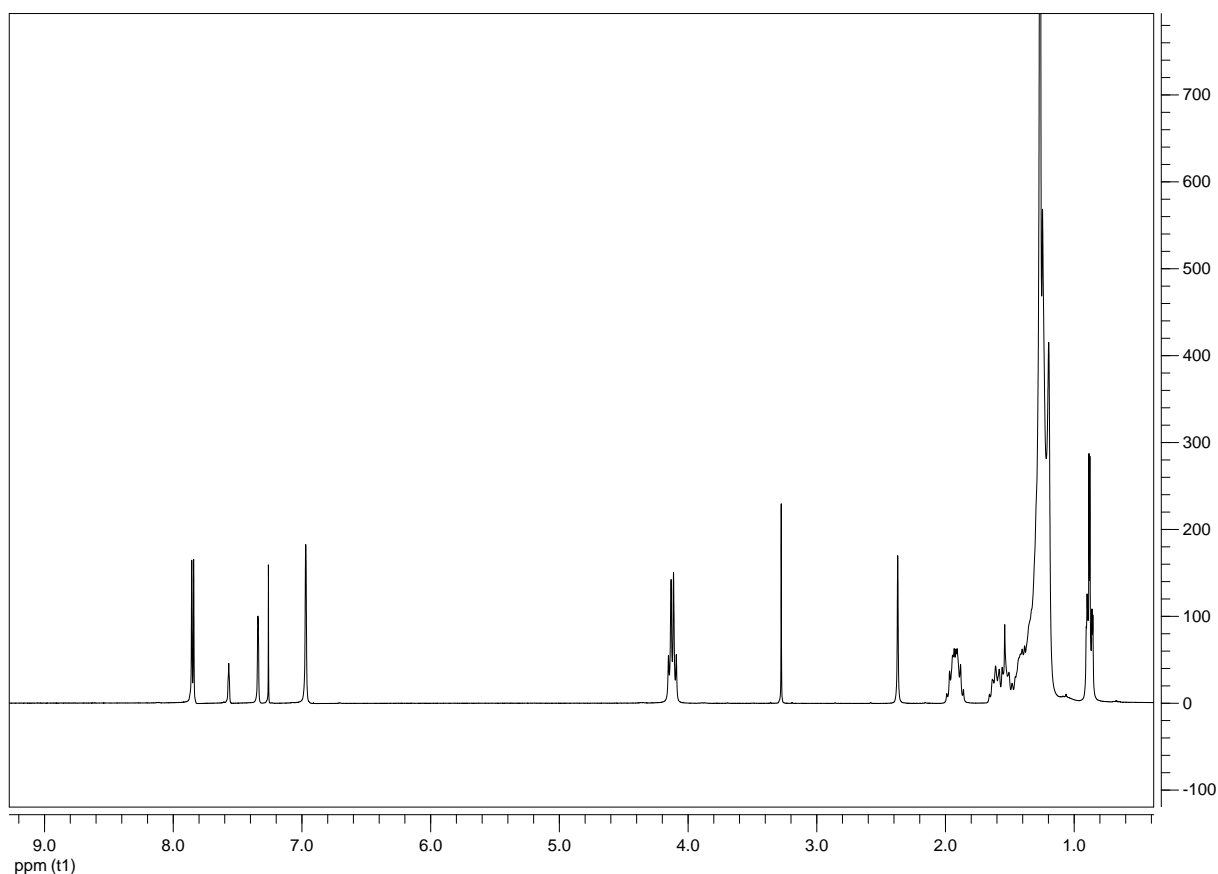


**Figure S43:**  $^1\text{H}$  NMR (300 MHz,  $\text{CDCl}_3$ ) of **12**.



**Synthesis of macrocycle 2.** The synthesis is performed according to the cyclization protocol developed in the synthesis of **3**. A 50 ml Hamilton syringe was charged with a solution of bisacetylene **12** (64.0 mg, 42.6  $\mu\text{mol}$ ) in THF (40 mL). Pd(PPh<sub>3</sub>)<sub>2</sub>Cl<sub>2</sub> (8.7 mg, 12.4  $\mu\text{mol}$ ) and CuI (6.5 mg, 34.1  $\mu\text{mol}$ ) together with 1,4-benzoquinone (18.0 mg, 166.5  $\mu\text{mol}$ ) were dissolved in THF (20 mL) and dry diisopropylamine (20 mL) and heated to 50 °C. While stirring vigorously, the acetylene-solution was added dropwise to the catalyst/oxidant-solution over a period of 72 h. The mixture was stirred for additional 48 h and subsequently diluted with CH<sub>2</sub>Cl<sub>2</sub> and water. The organic layer was extracted with water (2x), acetic acid (10 % v/v, 3x), NaOH (10 % w/w), and brine, and the solution was dried over MgSO<sub>4</sub>. The solvent was evaporated under reduced pressure. Inorganic compounds were removed by column chromatography (CH<sub>2</sub>Cl<sub>2</sub> : cyclohexane = 1 : 2, *R<sub>f</sub>* = 0.60). The resulting crude product was purified by preparative recycling GPC to yield **2** as a slightly yellow solid (21.3 mg, 7.04  $\mu\text{mol}$ , 33 %). M. p. 223 °C. <sup>1</sup>H NMR (500 MHz, CD<sub>2</sub>Cl<sub>2</sub>):  $\delta$  [ppm] = 7.94 (s, 4H), 7.88 (s, 4H), 7.68–7.66 (m, 2H), 7.31 (d, *J* = 0.64 Hz, 4H), 6.96 (s, 8H), 4.13 (m, 16H), 2.37 (s, 6H), 2.00–1.90 (m, 16H), 1.70–1.61 (m, 8H), 1.60–1.50 (m, 16H), 1.50–1.13 (m, 216H), 0.87 (t, *J* = 6.95 Hz, 24H). <sup>13</sup>C NMR (125 MHz, CDCl<sub>3</sub>):  $\delta$  [ppm] = 158.38, 158.04, 138.12, 136.11, 135.05, 133.36, 132.18, 131.82, 123.97, 123.12, 112.77, 111.60, 105.55, 105.35, 92.95, 86.33, 78.85, 78.04, 68.91, 68.69, 32.10, 29.88, 29.75, 29.54, 29.39, 29.07, 26.42, 26.15, 22.86, 21.29, 14.29. MALDI-MS (DCTB): *m/z* = 3022.5 (M<sup>+</sup>), C<sub>214</sub>H<sub>324</sub>O<sub>8</sub> requires 3022.49). GPC (PS calibration): single peak at *M*<sub>peak</sub> = 4.99 × 10<sup>3</sup> g mol<sup>-1</sup>.

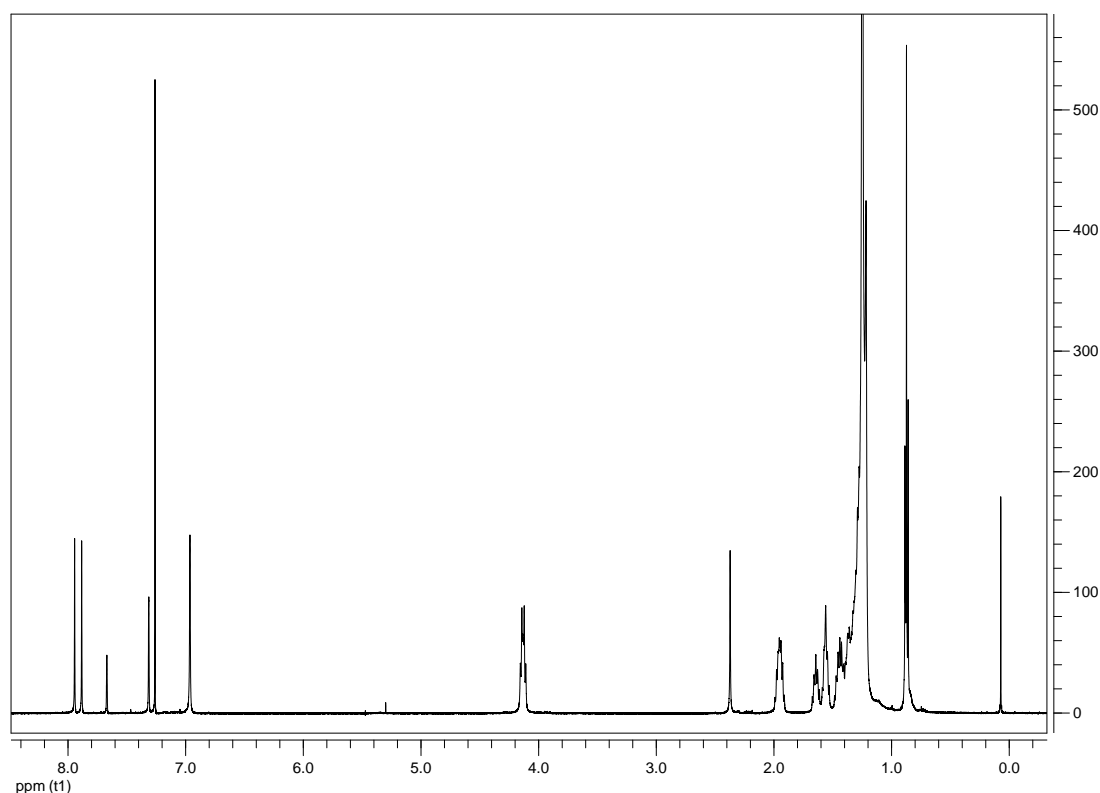


**Figure S45:** <sup>1</sup>H NMR (500 MHz, CDCl<sub>3</sub>) of **2**.

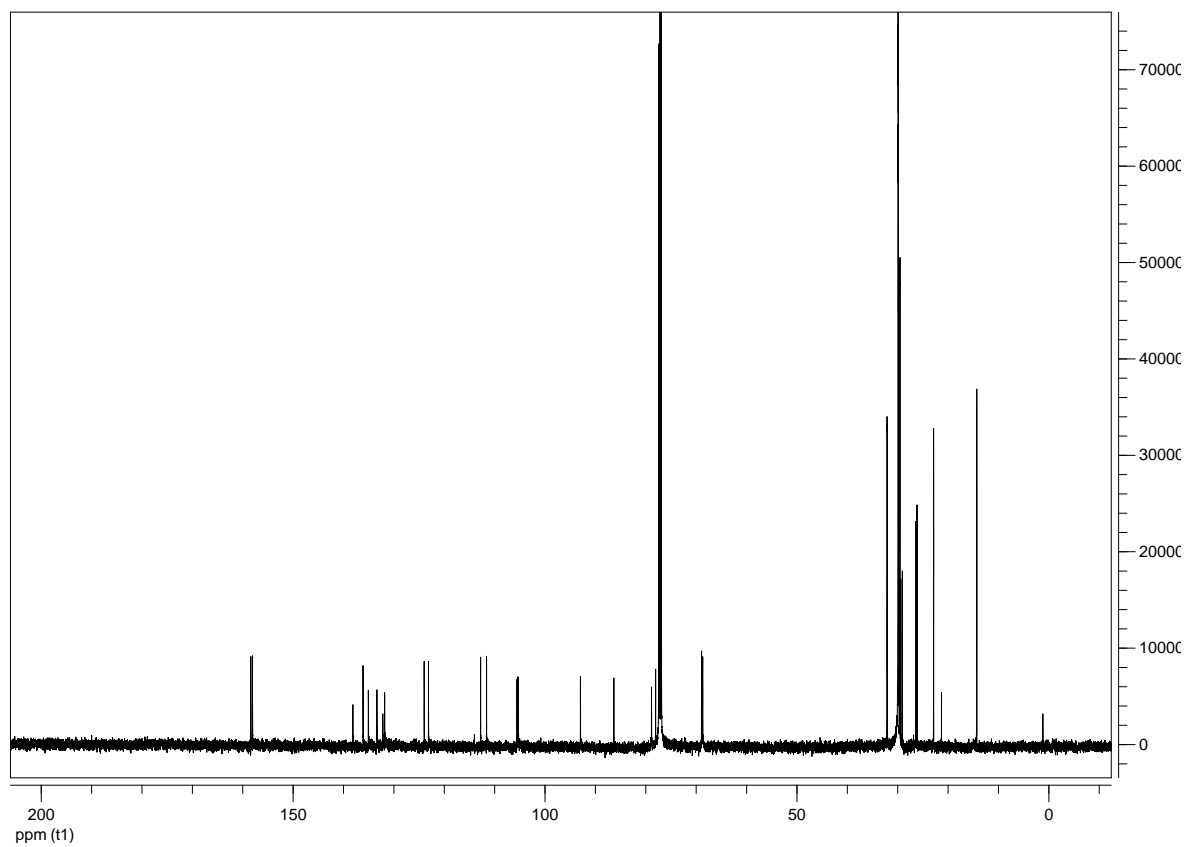


**Figure S46:**  $^{13}\text{C}$  NMR (125 MHz,  $\text{CDCl}_3$ ) of **2**.

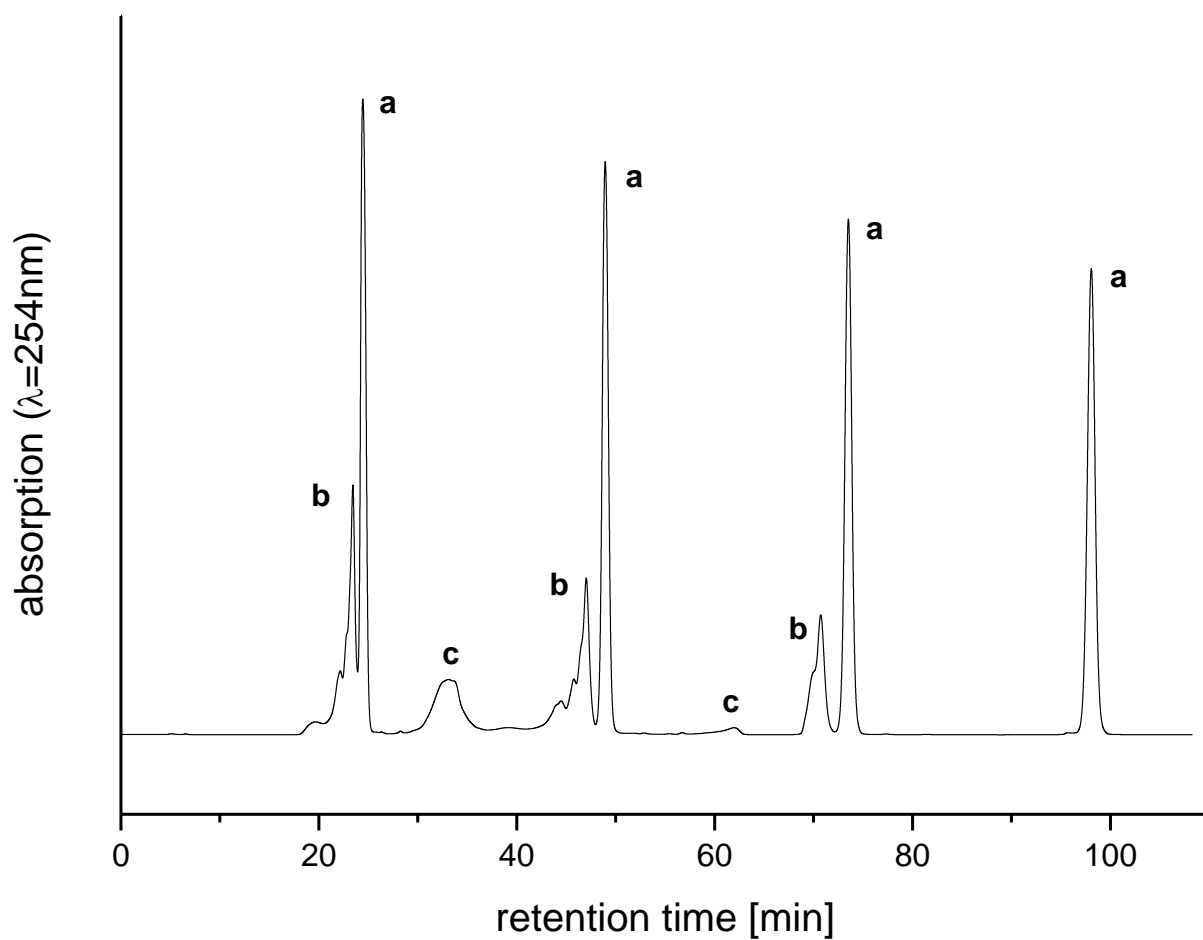


**Figure S47:** Recycling GPC elugram of the crude product of **2**. The macrocycle (signal **a**) is isolated from oligomeric byproduct (**b**) and further impurities (**c**) after four cycles.

## References

- [1] R. G. Cooke, B. L. Johnson, W. R. Owen, *Aust. J. Chem.* **1960**, *13*, 256-260.
- [2] A. Roedig, in: *Houben-Weyl*, Vol. 5, 4<sup>th</sup> Ed., Thieme, Stuttgart, **1960**, p. 517.
- [3] S. Höger, K. Bonrad, *J. Org. Chem.* **2000**, *65*, 2243-2245.
- [4] A. W. Williamson, *Quarterly Journal of the Chemical Society* **1852**, *4*, 229 - 239.
- [5] K. Sonogashira, Y. Tohda, N. Hagihara, *Tetrahedron Lett.* **1975**, *16*, 4467-4470.
- [6] a) S.-S. Jester, E. Sigmund, S. Höger, *J. Am. Chem. Soc.* **2011**, *133*, 11062-11065; b) S.-S. Jester, N. Shabelina, S. M. Le Blanc, S. Höger, *Angew. Chem. Int. Ed.* **2010**, *49*, 6101-6105; c) W. A. Chalifoux, R. McDonald, M. J. Ferguson, R. R. Tykwinski, *Angew. Chem.* **2009**, *121*, 8056-8060; d) P. Siemsen, Robert C. Livingston, F. Diederich, *Angew. Chem.* **2000**, *112*, 2740-2767.
- [7] a) S. Höger, A. D. Meckenstock, *Chem. Eur. J.* **1999**, *5*, 1686-1691; b) A. Ziegler, W. Mamdouh, A. Ver Heyen, M. Surin, H. Uji-i, M. M. S. Abdel-Mottaleb, F. C. De Schryver, S. De Feyter, R. Lazzaroni, S. Höger, *Chem. Mater.* **2005**, *17*, 5670-5683.
- [8] K. T. Potts, *Journal of the Chemical Society (Resumed)* **1953**, *42*, 3711-3712.
- [9] Q. Liu, D. J. Burton, *Tetrahedron Lett.* **1997**, *38*, 4371-4374.
- [10] V. E. Williams, T. M. Swager, *J. Polym. Sci., Part A: Polym. Chem.* **2000**, *38*, 4669-4676.